THE JOURNAL OF COMPARATIVE NEUROLOGY 458:221-239 (2003)

Reductions in N-Acetylaspartylglutamate and the 67 kDa Form of Glutamic Acid Decarboxylase Immunoreactivities in the Visual System of Albino and Pigmented Rats after Optic Nerve Transections

JOHN R. MOFFETT
Department of Biology, Georgetown University, Washington, DC 20057-1229

ABSTRACT

This study compares the immunohistochemical distributions of N-acetylaspartylglutamate (NAAG) and the large isoform of the y-aminobutyric acid (GABA)-synthesizing enzyme glutamic acid decarboxylase (GAD_{67}) in the visual system of albino and pigmented rats. Most retinal ganglion cells and their axons were strongly immunoreactive for NAAG, whereas GAD_{67} immunoreactivity was very sparse in these cells and projections. In retinorecipient zones, NAAG and GAD_{67} immunoreactivities occurred in distinct populations of neurons and in dense networks of strongly immunoreactive fibers and synapses. Dual-labeling immunohistochemistry indicated that principal neurons were stained for NAAG, whereas local interneurons were stained for GAD_{67}. In contrast to the distribution observed in retinorecipient zones, most or all neurons were doubly stained for NAAG and GAD_{67} in the thalamic reticular nucleus. Ten days after unilateral optic nerve transection, NAAG-immunoreactive fibers and synapses were substantially reduced in all contralateral retinal terminal zones. The posttransection pattern of NAAG-immunoreactive synaptic loss demarcated the contralateral and ipsilateral divisions of the retinal projections. In addition, an apparent transynaptic reduction in GAD_{67} immunoreactivity was observed in some deafferented areas, such as the lateral geniculate. These findings suggest a complicated picture in which NAAG and GABA are segregated in distinct neuronal populations in primary visual targets, yet they are colocalized in neurons of the thalamic reticular nucleus. This is consistent with NAAG acting as a neurotransmitter release modulator that is coreleased with a variety of classical transmitters in specific neural pathways. J. Comp. Neurol. 458:221-239, 2003.

Indexing terms: NAAG; immunohistochemistry; glutamic acid decarboxylase; GABA; lateral geniculate

The retinal projection pathways in mammals utilize excitatory amino acid neurotransmission to initiate postsynaptic activity in neurons of the primary visual target areas. Electrophysiological and pharmacological studies have implicated both N-methyl-D-aspartate (NMDA) and non-NMDA-type glutamate receptors in this transmission process (Kemp and Sillito, 1982; Crunelli et al., 1987; Sillito et al., 1990a,b; Van den Pol, 1991; Funke et al., 1991). Ultrastructural immunocytochemical studies have demonstrated high levels of glutamate immunoreactivity in synaptic terminals of retinal origin (Montero and Wenthold, 1989; Montero, 1990; Cardozo et al., 1991). A nervous system-specific dipeptide, N-acetylaspartylglutamate (NAAG), also is found in very high concentrations in the visual system of mammals, e.g., 3.86 *μmol/g* weight in the optic tract of monkeys (Molinar-Rode and Pasik, 1992). It

Grant sponsor: The National Eye Institute; Grant number: EY 09085.

Dr. John R. Moffett's current address is Uniformed Sciences University of the Health Sciences, Bethesda, MD 20814.

Correspondence to John R. Moffett: Uniformed Sciences University of the Health Sciences, Building C, Room 2109, 4301 Jones Bridge Road, Bethesda, MD 20814. E-mail: jmoffett@usuhs.mil

Received 23 May 2002; Accepted 25 September 2002

DOI 10.1002/cne. 10570

Published online the week of February 17, 2003 in Wiley InterScience (www.interscience.wiley.com).

is localized in most retinal ganglion cells; in the optic nerves, chiasm, and tracts; and in the neuropil of all retinal target areas (Tieman et al., 1987, 1988, 1991a; Anderson et al., 1987; Moffett et al., 1990). Optic nerve transection and eye removal experiments have demonstrated that NAAG is localized in the synaptic terminals of retinal ganglion cells (Moffett et al., 1991b; Tieman et al., 1991b), and release experiments have demonstrated the calcium dependence of NAAG release (Williamson and Neale, 1988; Tsai et al., 1988; Zollinger et al., 1988; Williamson et al., 1991). Extracellular peptidase activities hydrolyze the dipeptide into glutamate and another nervous system-specific acetylated compound, N-acetylaspartate (Serval et al., 1990; Thomas et al., 2000).

NAAG itself is a weak but selective agonist at NMDA receptors (Westbrook et al., 1986; Trombley and Westbrook, 1990; Sekiguchi et al., 1992; Valivullah et al., 1994). However, it does not produce consistent NMDA-mediated postsynaptic responses under several electrophysiological paradigms (Riveros and Orrego, 1984; Henderson and Salt, 1988; Whittemore and Koerner, 1989; Radhakrishnan and Henry, 1993). NAAG application, in the lateral geniculate nucleus (LG) of the cat, is reported to elicit slow, weak excitatory action on fewer than 50% of neurons, while having a weak inhibitory effect on approximately 10% of neurons tested (Jones and Sillito, 1992). For the suprachiasmatic nucleus, NAAG is reported to depolarize neurons and to potentiate the action of glutamate (Bos and Mirmiran, 1993). NAAG also has been implicated in the perception of chronic and neuropathic pain (Yamamoto et al., 2001).

NAAG inhibits forskolin-stimulated increases in neuronal cAMP through metabotropic glutamate receptors (Wroblewska et al., 1993). Current evidence indicates that NAAG acts specifically through the mGluR3 subtype of metabotropic glutamate receptor (mGluR) to reduce intracellular cAMP formation (Wroblewska et al., 1997, 1998). For example, in hippocampal slices, NAAG inhibits long-term potentiation at the perforant-granule cell synapse via mGluR3 receptor-mediated reductions in cAMP formation (Lea et al., 2001). NAAG is also neuroprotective, probably via mGluR activation (Bruno et al., 1998a; Lu et al., 2000; Thomas et al., 2000).

NAAG affects the release of classical transmitters, including stimulation of dopamine release in the striatum and substantia nigra (Galli et al., 1991) and inhibition of norepinephrine release in the hippocampus (Puttfarcken et al., 1993). Furthermore, NAAG inhibits KC1-stimulated [^{3}H]γ-aminobutyric acid (GABA) release from cortical interneurons (Zhao et al., 2001), and this inhibition was correlated with mGluR3-mediated reductions in cAMP and subsequent reductions in protein kinase A activity and L-type calcium channel conductance. These findings have led Neale et al. (2000) to hypothesize that NAAG acts predominantly at presynaptic mGluR3 receptors to modulate further transmitter release. Taken together, the mounting evidence on NAAG's actions in the nervous system strongly implicate this molecule in presynaptic neurotransmitter release modulation by reducing cAMP formation through the mGluR3 receptor. Low-level activation of some glutamatergic systems may also be one of NAAG's actions in the nervous system, but this action is less well established in vivo.

By utilizing a significantly improved fixation procedure for NAAG immunohistochemistry (Moffett et al., 1993, 1994) and highly purified antibodies (Moffett and Namboodiri, 1995), a detailed analysis was made of the distribution of this dipeptide throughout the visual system of both pigmented and albino rats 10 days after unilateral or bilateral optic nerve transections. The results obtained using the new methods were improved in several ways compared with previous studies of NAAG localization in the visual system. The newer methods provided dramatically greater detail in the staining of cellular and neuropil elements; comprehensive axonal labeling, which was not possible using previous methods lacking the dimethylsulfoxide (DMSO) penetrant; greatly reduced background staining; and uniform NAAG labeling throughout the brain. With these new methods, the first detailed comparison was made in the rat visual system between the distribution of NAAG and that of the 67 kDa form of glutamic acid decarboxylase (GAD_{67}), a marker for inhibitory neurons that utilize GABA as a neurotransmitter. This study also provides the first comparison of the visual projections in albino and pigmented rats using antibodies to both NAAG and GAD.

MATERIALS AND METHODS

Chemicals were from Sigma (St. Louis, MO), except where otherwise noted. Solutions were prepared with purified water. Normal goat serum (NGS), horseradish peroxidase (HRP)-labeled avidin-biotin complex, biotinylated secondary antibody, and HRP-labeled secondary antibody reagents were from Vector (Burlingame, CA). Polyclonal rabbit antibodies to GAD_{67} were from Chemicon (Temecula, CA; K2 antibody), and additional HRP-labeled goat anti-rabbit secondary antibodies were from Kirkegaard and Perry (Gaithersburg, MD). Animals were from, and surgery and postoperative care were performed by, Zivic Miller (Zelienople, PA). Research was conducted in compliance with the *Guide for the Care and Use of Laboratory Animals* (NIH publication 85-23) and the Georgetown University Animal Care and Use Committee. Polyclonal antibodies to NAAG were produced in rabbits and were affinity purified and negative-affinity adsorbed as previously described (Moffett et al., 1994). Nitrocellulose-immobilized protein conjugates of N-acetylaspartate, glutamate, aspartate, N-acetylglutamate, and GABA as well as carbodiimide-treated whole brain proteins were used as adsorbants. The specificity of the NAAG antibodies has been described previously (Moffett and Namboodiri, 1995).

Sprague-Dawley albino and Long-Evans pigmented (hooded) male rats, weighing between 130 and 180 g, were used for this study. They included six albino rats with preretinal (intraorbital) unilateral optic nerve transections, two albino rats with intracranial unilateral optic nerve transections, five hooded rats with preretinal unilateral transections, and six hooded rats with preretinal bilateral optic nerve transections. Three albino and three hooded rats without operations were also examined. Ten days after optic nerve transections, animals were deeply anesthetized with pentobarbitol (300 mg/kg) according to approved animal care and use protocols and were perfused transcardially with 500 ml of an aqueous solution of 6% l-ethyl-3(3-dimethylaminopropyl)carbodiimide hydrochloride (EDAC) containing 6% (n = 21) or 10% (n = 4) DMSO and 1 mM N-hydroxysuccinimide, as previously described (Moffett et al., 1993, 1994). Brains and eyes

were removed to a solution of 100 mM sodium phosphate in physiological saline at pH 8 containing 4% formaldehyde for 24-48 hr. The tissue was serially saturated with 10%, 20%, and 30% sucrose solutions in phosphate-buffered saline (PBS; pH 7.2) prior to freezing. Brains were sectioned in the frontal plane from the anterior preoptic area to the anterior pons at a thickness of 20 |jim, and retinas were cut in cross section at a thickness of 30 jjim.

Tissue sections were incubated with 2% NGS in PBS (pH 7.2, containing 0.1% sodium azide) for 30 minutes or longer before applying antibody. Brain sections were processed freely floating in 30 mm tissue culture dishes, whereas retinal sections were mounted on slides before staining. Purified anti-NAAG antibodies were diluted 1:200 to 1:400 (relative to the volume of crude serum) in PBS with 2% NGS and incubated with sections for 48 hr or longer at room temperature under constant rotary agitation in a humid chamber. Antibodies to GAD_{67} were diluted from 1:14,000 to 1:16,000 and incubated with adjacent tissue sections under the same conditions. Bound antibodies were visualized by the avidin-biotin complex method with peroxidase as the marker enzyme. The biotinylated secondary antibodies and avidin-HRP complex solutions were each incubated with tissue sections for 80-90 minutes, with four washes of PBS between. After final washing, the sections were developed with an Ni and Co enhanced diaminobenzidene/peroxide reaction (Pierce Chemical Co., Rockford, IL). The sections were mounted on treated slides (Superfrost Plus; Fisher Scientific, Pittsburgh, PA), dried, dehydrated in an ethanol series, and covered with xylene and resin.

Dual-labeling immunohistochemistry was performed sequentially for the two antigens. NAAG antibodies (1:200 to 1:400) were incubated with the sections for 48 hr and processed as described above. The chromogen employed in the first stage of staining was diaminobenzidene with catechol (HistoMark Orange; Kirkegaard and Perry), which produces an orange reaction product. The HRP marker enzyme used to visualize the first antigen was then inhibited by incubating sections for 30 minutes in 50:50 methanol/water containing 1% H_20_2 and 10 mM dithiothreitol. Sections were washed thoroughly with PBS and incubated for 30 minutes in 2% NGS in PBS. The sections were then incubated with GAD_{67} antibodies overnight (1:6,000 to 1:7,000 in 2% NGS), with constant agitation. The antibodies to GAD_{67} were detected with HRP-labeled goat anti-rabbit secondary antibodies (Kirkegaard and Perry) at a concentration of 5 µg/ml in PBS containing 0.2% bovine serum albumin (90 minute incubation). Sections were washed thoroughly in PBS and developed with a purple chromogen (VIP; Vector).

Control experiments were carried out to ensure that no primary (rabbit) anti-NAAG antibodies from the first incubation were detected by the labeled secondary (goat anti-rabbit) antibodies used in the localization of GAD_{67}. Sections were incubated for 48 hr in NAAG antibodies (1:200 in 2% NGS) and processed as usual for dual labeling, but they were not developed with chromogen. The peroxidase marker was inhibited as noted above, and then the sections were processed for a second antigen as described above, with the exception that the GAD_{67} antibodies were excluded, and, instead, the sections were incubated for 24 hr with 2% NGS. The sections were then washed and incubated for 90 minutes with 5 µg/ml HRP-labeled goat anti-rabbit secondary antibodies and developed with the Ni/Co enhanced chromogen. Other standard control tests for antibody specificity were also performed as previously described (Moffett and Namboodiri, 1995).

The neuroanatomical nomenclature used in this study was taken from Swanson (1992). The photomicrographs were taken on 35 mm Kodak color Kodachrome ASA 25 film or Tmax ASA 100 black-and-white film, with a Zeiss Axiophot microscope, and digitally scanned using a Nikon Coolscan II film scanner (1,350 dpi). Black-and-white digitized images were not corrected for contrast or brightness, but color images were color corrected when necessary using PC-based imaging software.

RESULTS

Enhanced carbodiimide fixation (Moffett et al., 1993) provided a significant improvement in the immunohistochemical localization of NAAG in the rat visual system compared with previous studies. Greater cellular and neuropil detail and dramatically improved axonal labeling permitted a detailed analysis of the localization of this dipeptide throughout the retinal projections. Two concentrations of DMSO were used to increase fixative penetration into tissues. The higher concentration of DMSO (10%), was found to produce fixation artifacts and excessive tissue shrinkage but did not alter the overall pattern of immunoreactivity. The lower concentration (6%) yielded excellent results both in terms of uniform staining for NAAG throughout the tissue and in terms of good tissue preservation. Tissue shrinkage was still apparent but was not excessive. The use of nickel and cobalt to enhance the opacity of the diaminobenzidene reaction product provided additional sensitivity for fine processes and puncta.

Highly specific antibodies to NAAG were made possible by several purification steps. Antibodies were first incubated with nitrocellulose-bound protein (bovine serum albumin) conjugates of several molecules, including glutamate, aspartate, N-acetylglutamate, N-acetylaspartate, and GABA, as well as with immobilized carbodiimide-treated rat brain proteins. This initial "negative-affinity adsorption" step was followed by affinity purification (Moffett et al., 1994). After affinity purification, anti-NAAG antibodies were tested for specificity against serial dilutions of the conjugates listed above. If any remaining cross reactivities were observed, the antibodies were again incubated overnight with the nitrocellulose-bound protein conjugates until assays showed no remaining cross reactivity (Moffett and Namboodiri, 1995).

The results obtained with the combined use of these new methods were improved over results from previous studies in several ways, including 1) greater cytological detail, 2) comprehensive axonal labeling, 3) reduced background staining, and 4) uniform labeling across areas. The lack of penetrant in previous studies of the visual system limited the ability to demonstrate clearly the loss of staining in fiber pathways after optic nerve section. In addition to the improvements in NAAG immunolabeling, this study is the first detailed analysis of the differences in NAAG and GAD staining in the visual projections of albino and pigmented rats.

In general, NAAG immunoreactivity (NAAG-IR) was punctate in nature, often appearing as densely packed puncta throughout the somata and proximal dendrites of neurons. NAAG staining was never seen in the distal dendritic branches of immunoreactive neurons. Intense

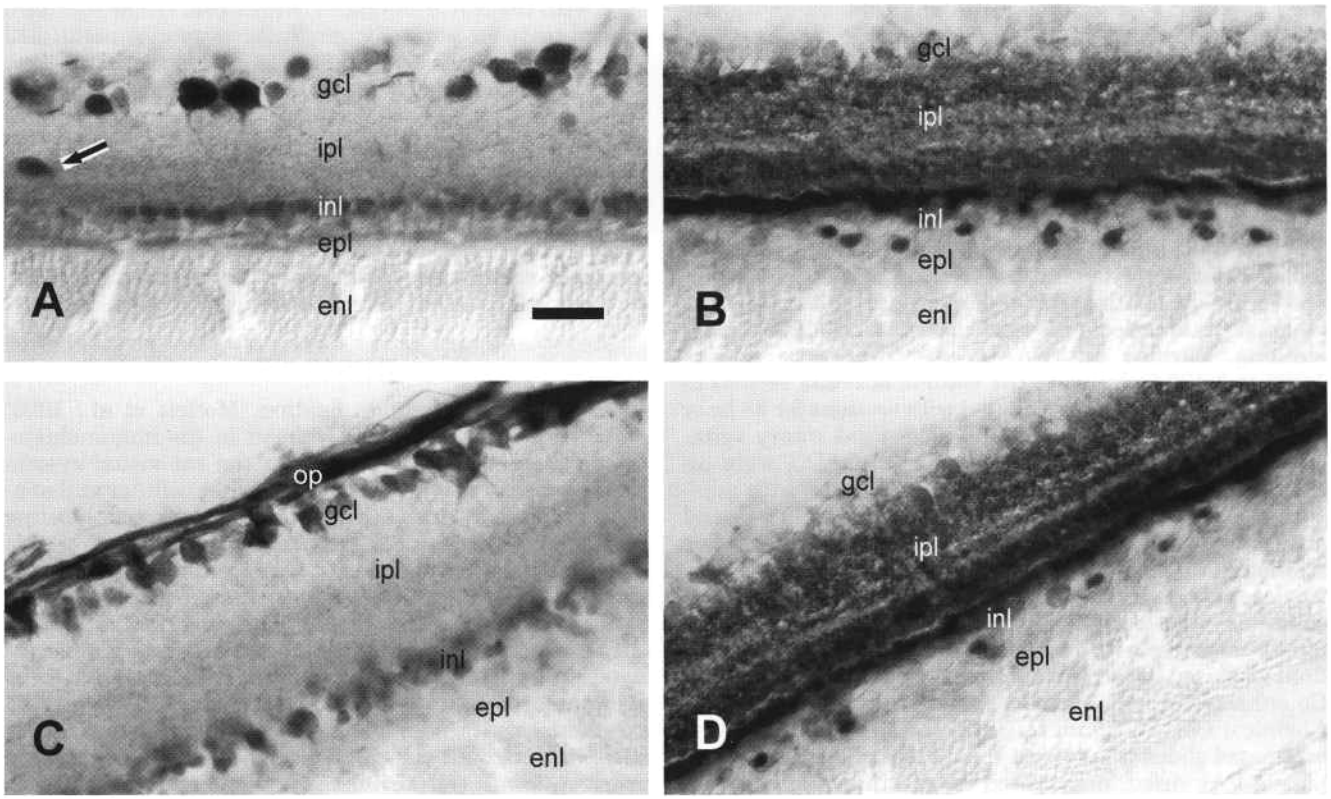

Fig. 1. NAAG-IR and GAD_{67}-IR in the albino rat retina. NAAG-IR (A,C) was observed in many, but not all, neurons of the ganglion cell layer (gcl). Occasional neurons in the inner plexiform layer (ipl) were also stained for NAAG (arrow in A). Neurons concentrated on the inner margin of the inner nuclear layer (inl) were moderately stained for NAAG, whereas photoreceptor cells of the external nuclear layer (enl) were not stained. Patchy, light NAAG-IR was present in the external plexiform layer (epl in A). Light to moderate punctate NAAG-IR was observed in the ipl neuropil, with higher levels in the more superficial layers bordering the inl. Most or all axons within the optic fiber layer (op in C) were intensely stained for NAAG. GAD_{67}-IR in the rat retina was observed in a population of neuronal cell bodies in the inl and in a dense network of strongly stained puncta concentrated in several longitudinal bands within the neuropil of the ipl (B,D). GAD_{67}-immunoreactive neurons in the inl were scattered throughout the layer, unlike NAAG-IR neurons, which were selectively localized to the border with the ipl. Many neurons in the gcl exhibited light, punctate GAD_{67}-IR on their surfaces, suggestive of synaptic contacts. Scale bar = 20 μm.

axonal staining occurred in specific neural pathways, such as the retinal ganglion cell projections, but not all NAAG-positive cell groups had immunopositive efferent fiber tracts. For example, the somata of neurons in the thalamic reticular nucleus were all strongly positive for NAAG and GAD, but their GAD-positive axons in the internal capsule were never stained for NAAG. The new fixation method employing a penetrant ensured that NAAG could be detected throughout fiber pathways, so the lack of immunoreactivity in certain projections was not due to incomplete fixation of NAAG in white matter.

Retina

As observed in previous studies (Anderson et al., 1987; Moffett et al, 1991b; Williamson et al, 1991), NAAG-IR in the retina was most prominent in retinal ganglion cells (Fig. 1A,C). No differences in immunoreactivity were observed between albino and hooded rat retinas. Most of the cells in the ganglion cell layer were immunoreactive for NAAG, with cells ranging from lightly to intensely stained. All size classes of ganglion cells were stained for NAAG, and no relationship was observed between staining intensity and the size of the neuronal somata. The proximal dendrites of some ganglion cells could be seen entering multiple sublayers of the inner plexiform layer. Most ganglion cell axons within the optic fiber layer were strongly stained for NAAG (Fig. 1C). NAAG-immunoreactive puncta occurred throughout the inner plexiform layer, being more concentrated near the inner nuclear layer. NAAG-immunoreactive neuronal somata were present in the inner nuclear layer, particularly along the border with the inner plexiform layer (Fig. 1A,C). Very light punctate NAAG-IR was observed in the external plexiform layer of the retina. Photoreceptor cells with cell bodies in the external nuclear layer were the only cell type in the retina that never stained for NAAG.

GAD_{67}-IR in the rat retina was intense in scattered neuronal cell bodies in the inner nuclear layer and within the neuropil of the inner plexiform layer, where staining was concentrated in several longitudinal bands (Fig. 1B,D). GAD_{67}-IR was also associated with the surface of neurons in the ganglion cell layer, suggestive of GAD-containing synaptic contacts. A very small number of neurons in the ganglion cell layer contained moderate immunoreactivity for GAD_{67} throughout their cytoplasm, possibly representing displaced amacrine cells. However,

no GAD_{67}-IR occurred in axons in the optic fiber layer or in photoreceptor cells in the external nuclear layer.

Optic chiasm and suprachiasmatic nucleus

Most or all of the axons of the optic nerves were immunoreactive for NAAG in both albino and pigmented rats (Fig. 2A). The optic chiasm from a pigmented rat is shown in Figure 2B stained for NAAG 10 days after unilateral transection at several rostrocaudal levels. In the animals with unilateral optic nerve transections, the loss of NAAG-IR in the optic chiasm produced a staining pattern very similar to that observed following injection of tracer compounds into one eye (Fig. 2B; Kita and Oomura, 1982; Johnson et al., 1988). When bilateral optic nerve transections were performed, all immunoreactivity was lost in the optic nerves (data not shown). However, a belt of NAAG-immunoreactive fibers remained below the optic chiasm, as can be seen in Figure 3B. These fibers made up the supraoptic commissure and were not directly associated with the retinal projections.

NAAG-IR in the suprachiasmatic nucleus (SCN) was observed in both neurons and neuropil (Fig. 3A,C,E). Neurons with NAAG-IR occurred throughout the SCN, but those with the highest degree of immunoreactivity were located in the dorsomedial aspect of the caudal portion of each nucleus. Immunoreactivity for NAAG in the neuropil was also observed throughout the SCN, but the density of NAAG-immunoreactive puncta was notably greater in a relatively restricted zone in the ventrolateral quadrant of the posterior half of the nucleus (Fig. 3A,C). The NAAG-IR in this neuropil was present in very fine puncta that could be observed only at high magnification (Fig. 3E). Much of the punctate NAAG-IR in the ventrolateral neuropil was lost in both SCN after bilateral optic nerve transections (Fig. 3B,D,F).

GAD_{67}-immunoreactive fibers were not observed in the optic nerves and chiasm. However, GAD_{67}-IR was very strong in the SCN neuropil, as previously reported (Moore and Speh, 1993), but was difficult to detect in cell bodies. After unilateral and bilateral optic nerve transections, changes in GAD_{67}-IR in the SCN were not apparent (data not shown).

LG and optic tract

The LG was conspicuous in NAAG-stained sections, containing substantially greater NAAG-IR than surrounding thalamic nuclei (see Fig. 4B). Immunoreactivity for NAAG in the optic tract of albino and pigmented rats was intense in the majority of axons, and these were observed entering the LG at all levels (Fig. 4B). NAAG-immunoreactive fibers diverged from the optic tracts to penetrate both the dorsal LG (LGd) and the ventral LG (LGv). The supraoptic commissure runs adjacent to the optic tracts at the level of the LG, and most of its fibers were stained moderately for NAAG. Scattered NAAG-immunoreactive neurons were intercalated within the supraoptic commissure.

NAAG-stained elements were extensive in the rat LGd and included axons, terminals, and somata of principal LGd neurons. NAAG-immunoreactive fibers formed numerous terminals of various sizes in the LGd and LGv, many terminals in the LGd being exceptionally large and concentrated in clusters. The principal neurons of the LGd were moderately immunoreactive for NAAG, but their dendrites and the axons forming the cortical projections were unstained. In the animals with unilateral optic nerve transections, NAAG-IR was reduced to only a few scattered fibers in the optic tract contralateral to the cut nerve. The loss of NAAG-IR in the neuropil of the contralateral LGd observed 10 days after unilateral optic nerve transection was extensive (Fig. 4A). A patch of NAAG-immunoreactive puncta remained in the core region of the contralateral LGd that receives input from the ipsilateral eye (Fig. 4C). The homotopic core region in the opposite LGd (ipsilateral to the cut nerve) contained only sparse NAAG-immunoreactive puncta (Fig. 4D), whereas the surrounding geniculate body retained its strong NAAG-immunoreactive afferentation (Fig. 4B,D).

The ventral division of the lateral geniculate (LGv) contained cells and neuropil that were immunoreactive for NAAG (Fig. 5F,H). The medial division of the LGv was characterized by low NAAG-IR in the neuropil and strong NAAG-IR in medium-sized to large neuronal somata. Less intense NAAG-IR was observed in neurons with smaller somata. A very dense plexus of NAAG-IR puncta was present in the lateral subdivision of the LGv. After unilateral optic nerve transections, large reductions in NAAG-IR were observed in the neuropil of the lateral portion of the contralateral LGv (Fig. 5E,G). A vertically oriented strip of NAAG-IR remained at the outer boarder of the LGv contralateral to the cut optic nerve. This remaining ipsilateral projection was more prominent in pigmented than in albino rats (cf. Fig. 5E and G). No noticeable changes in NAAG-IR occurred in the medial LGv after optic nerve transections.

GAD_{67}-IR was very limited in the optic tract of albino and pigmented rats (Fig. 4E,F). Sparse GAD_{67}-immunoreactive fibers and very small numbers of stained neurons were visible in the optic tracts. The supraoptic commissure, which courses adjacent to the optic chiasm and tracts, contained substantially more GAD_{67}-immunoreactive fibers and neuronal somata. In the LGd, many GAD_{67}-immunoreactive neurons were observed, with somata that were generally smaller than those with NAAG-IR in the same area. Ten days after unilateral optic nerve transections, a reduction in GAD_{67}-IR was observed in the LGd, with a pattern similar to that of the loss observed for NAAG-IR (Fig. 4E-H). In pigmented rats, a patch of higher GAD_{67}-IR was observed in the core of the LGd contralateral to the cut optic nerve, in the same position as was observed with the remaining NAAG-immunoreactive puncta (Fig. 4E). The loss of GAD_{67}-IR in the deafferented LGd appeared to be accompanied not by a reduction in the number df immunoreactive neuronal somata but rather by lower levels of immunoreactivity in the interneurons and associated neuropil in the denervated regions.

GAD_{67}-IR in the neuropil of the LGv was much more intense than that in the LGd. In the lateral portion of the LGv, a very dense network of GAD_{67}-immunoreactive puncta was present along with some strongly stained neurons with small cell bodies. The GAD_{67}-immunoreactive puncta were less dense in the medial LGv, and no immunoreactive somata were observed there. No observable reduction in GAD_{67}-IR occurred in the LGv after optic nerve transections (data not shown).

NAAG-IR in albino and pigmented retinogeniculate projections

After unilateral optic nerve transections, the distribution of NAAG-IR in the LGd of hooded rats exhibited the

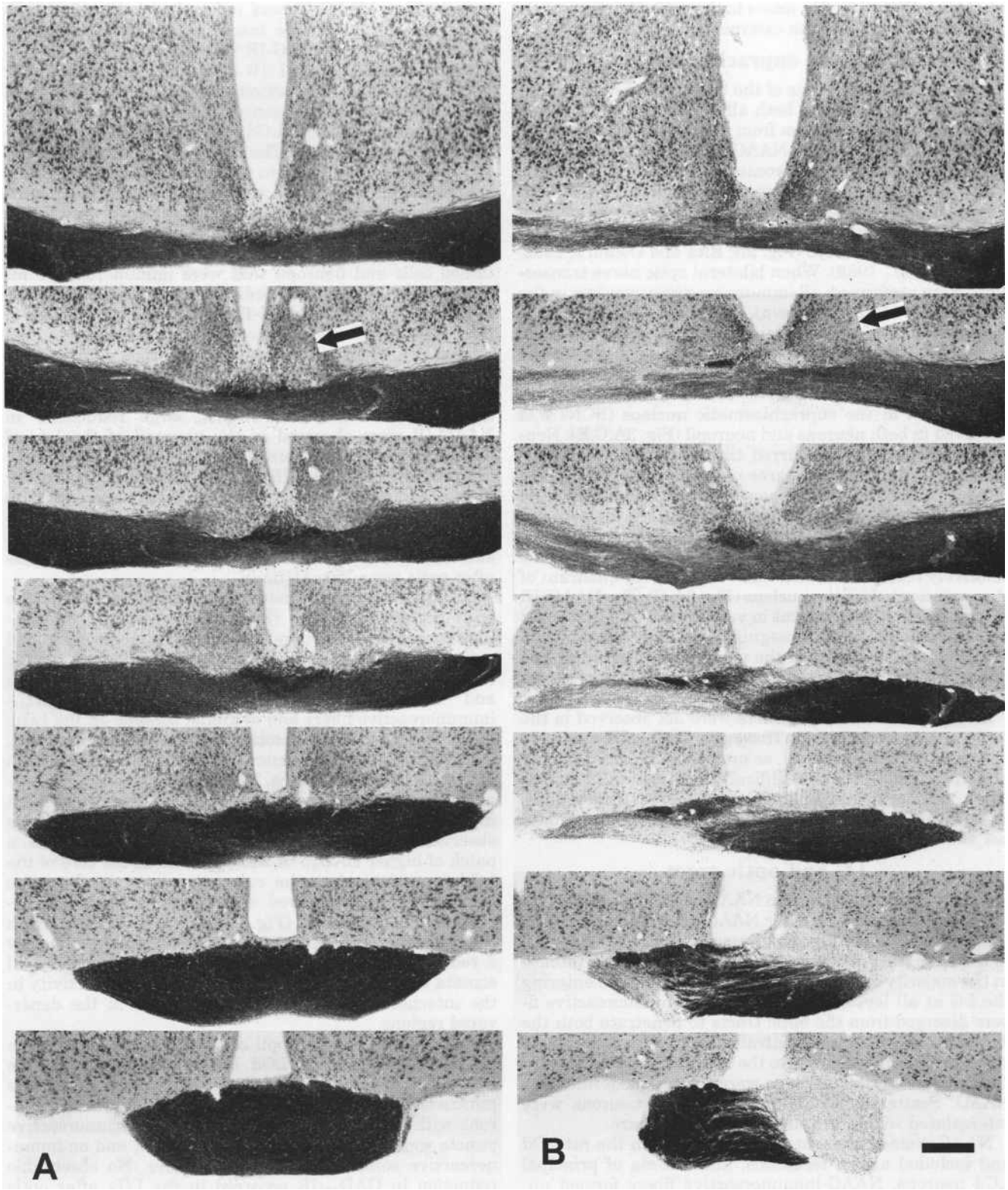

Fig. 2. NAAG-IR in the hooded rat optic chiasm. A montage is shown in A that depicts the optic chiasm and SCN (arrows) of a control hooded rat at several rostrocaudal levels. The sections are arranged in order from rostral at the bottom to caudal at the top. The staining pattern for NAAG in the optic chiasm of another pigmented rat is shown 10 days after unilateral optic nerve transection at similar rostrocaudal levels (B). The NAAG-IR fibers from the intact optic nerve can be seen crossing from one side of the chiasm to the other in the rostral sections (B). Scale bar = 300 μm.

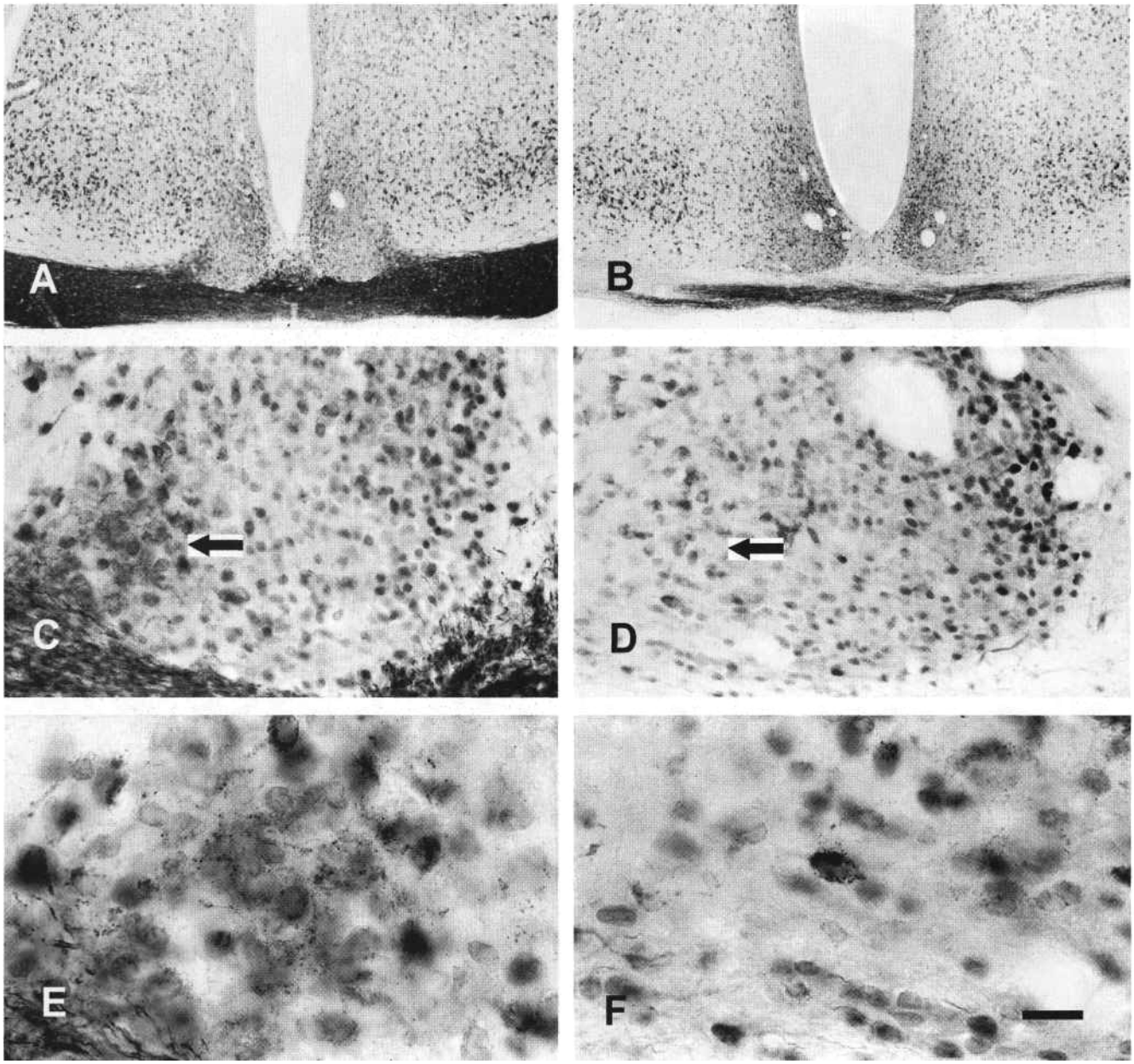

Fig. 3. NAAG-IR in the SCN of a control rat and a rat with bilateral optic nerve transections. NAAG-IR in the SCN of control rats was observed in both neurons and neuropil (shown at increasing magnification in A,C,E). Neurons with NAAG-IR were observed throughout the SCN, but those with the highest degree of immunoreactivity were located in the dorsomedial aspect of each nucleus. Immunoreactivity for NAAG was also observed in neuropil throughout the SCN, but the density of NAAG-IR puncta was much greater in a relatively restricted zone in the ventrolateral quadrant of the posterior half of the nucleus (arrows). NAAG-IR in the axons of the optic chiasm and the punctate NAAG-IR in the ventrolateral neuropil were lost in both SCN after bilateral optic nerve transections (shown at increasing magnification in B,D,F). The remaining NAAG-IR fibers at the base of the optic chiasm in (B) are stained axons of the supraoptic commissure and are not part of the retinal projections. Scale bar = 300 μm for A,B, 50 μm for C,D, 20 μm for E,F.

characteristic pattern of "core" and "shell" retinal terminal fields from opposing eyes (Figs. 4A,B, 5A,B)- The core region of the rat LGd receives retinal input from the ipsilateral eye, whereas the remaining shell of the LGd receives input from the contralateral eye. After a unilateral optic nerve transection, a large patch of NAAG-immunoreactive terminals was present in the dorsomedial LGd contralateral to the cut optic nerve, representing the remaining retinogeniculate terminals from the intact ipsilateral optic nerve (Figs. 4A, 5A). The corresponding central position in the opposite LGd was almost devoid of NAAG-immunoreactive puncta (Figs. 4B, 5B). This terminal distribution pattern from opposing eyes was less apparent in the LGd of albino rats after unilateral optic nerve transection (Fig. 5C,D) but could still be discerned. A similar distinction in the retinal terminal distribution

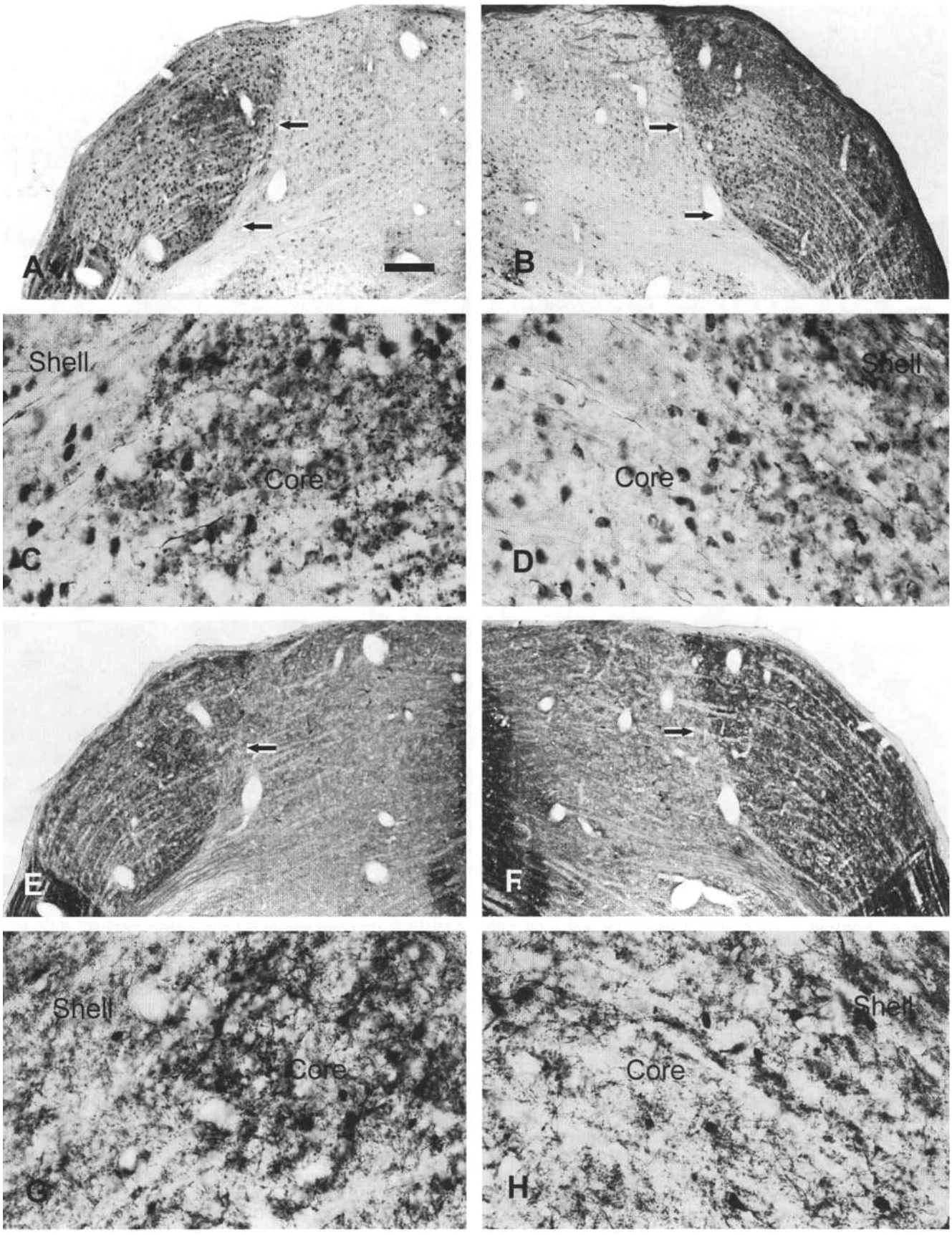

Figure 4

pattern in the LGv of albino and hooded rats was observed after unilateral optic nerve transections. In the lateral portion of the LGv of pigmented rats, clusters of NAAG-immunoreactive puncta remained contralateral to the cut optic nerve (Fig. 5E), whereas NAAG-IR in the neuropil remained strong ipsilateral to the cut nerve (Fig. 5F). In the LGv of albino rats, these remaining clusters of NAAG-immunoreactive puncta, representing the ipsilateral retinal projection to the LGv, were much less evident (Fig. 5G,H).

Pretectal nuclei and the nucleus of the optic tract

NAAG-immunoreactive axons of the optic tract were continuous with those of the brachium of the superior colliculus, which forms the roof of the pretectal area (Fig. 6B). Small bundles of NAAG-stained fibers were also observed exiting the dorsomedial aspect of the LGd and coursing caudally and medially toward the pretectal nuclei and nucleus of the optic tract (NOT). These NAAG-immunoreactive fibers passed through the lateral dorsal thalamic and anterior pretectal nuclei, ventral to the brachium of the superior colliculus. NAAG-immunoreactive fibers of the brachium of the superior colliculus, and the bundles ventral to it, could be observed distributing immunopositive terminals to the pretectal nuclei.

Ten days after a unilateral optic nerve transection, most of the NAAG-immunoreactive fibers in the brachium of the superior colliculus and those observed exiting the LGd in bundles were lost contralaterally to the transection (Fig. 6A). However, scattered fibers that were immunoreactive for NAAG could still be observed on the contralateral side. NAAG-IR in the olivary pretectal nucleus (OP) was observed predominantly in the neuropil (Fig. 6B). The anterior OP appeared as a dense oval of medium- and fine-grained NAAG-immunoreactive puncta. NAAG-IR was less prominent in the neuropil of the posterior OP, where some neurons were moderately stained for NAAG. Dense clusters of strongly NAAG-immunoreactive puncta were observed in the posterior pretectal nucleus (PPT; Fig. 6B). NAAG-IR in the neuropil of the PPT was observed in patches or clumps, as opposed to the even distribution observed in the OP. In addition, many PPT neurons were moderately to strongly stained for NAAG. In coronal sections, immunoreactive fibers could be seen entering the NOT from the brachium of the superior colliculus (Fig. 6B). The distribution of NAAG-immunoreactive puncta in the neuropil was highly clustered, even moreso than in the case of the PPT. NAAG-IR in the NOT was also observed in some neuronal somata (see Fig. 6A). In hooded rats with unilateral optic nerve transections, the punctate NAAG-IR in the neuropil of the OP was significantly reduced contralaterally to the cut nerve (Fig. 6A). In albino rats with unilateral optic nerve transections, the contralateral loss of NAAG-immunoreactive puncta was almost complete (data not shown). After unilateral optic nerve transections in both strains of rat, NAAG-IR in the neuropil of the PPT and NOT was similar to that in control rats ipsilateral to the cut nerve (Fig. 6B) but was nearly absent contralateral to the cut nerve (Fig. 6A).

GAD_{67}-IR in the pretectal nuclei was observed in small neuronal somata, fibers, and puncta. In the OP, PPT, and NOT, GAD_{67}-IR was present in a network of fine fibers and puncta and in numerous small neurons (Fig. 6D). Ten days after unilateral optic nerve transection, GAD_{67}-IR was reduced in the contralateral NOT (Fig. 6C). In contrast, there was little or no reduction in GAD_{67}-IR in the OP or PPT (Fig. 6C).

Lateral and dorsal terminal nuclei of the accessory optic tract

The lateral terminal nucleus (LTN), located ventrally to the caudal pole of the LG, contained strong NAAG staining in fibers, puncta, and somata (Fig. 7B). The dorsal terminal nucleus (DTN), a small retinorecipient area located superficially between the superior colliculus (SC) and the medial geniculate body, exhibited NAAG-IR in the neuropil. Some immunoreactive neurons were observed surrounding the nucleus (Fig 7F). Ten days after unilateral optic nerve transection, NAAG-IR was nearly eliminated in fibers and synapses in the LTN and DTN contralateral to the cut nerve (Fig. 7A,E).

GAD_{67}-IR was present in the neuropil and some small neuronal somata in both the LTN (Fig. 7D) and the DTN (Fig. 7H). No detectable loss of GAD_{67}-IR was observed in either nucleus following deafferentation (Fig. 7C,G).

NAAG-IR and GAD_{67}-IR in the medial terminal nucleus

The medial terminal nucleus (MTN) of the accessory optic tract, located medially to the substantia nigra, contained dense fibers and puncta that were strongly immunoreactive for NAAG in the dorsal and ventral subdivisions (Figs. 8B, 10H). After unilateral optic nerve transections in both albino and hooded rats, most of the NAAG-IR in the neuropil of the MTN was lost contralaterally to the cut optic nerve (Figs. 8A, 10G).

In the MTN, GAD_{67}-IR was present in a dense plexus of fibers and puncta and in scattered small neurons (Fig. 8D). A slight reduction in the intensity of GAD_{67}-IR was observed in the contralateral MTN after unilateral optic nerve transection (Fig. 8C).

Fig. 4. NAAG-IR and GAD_{67}-IR in the hooded rat LGd after unilateral optic nerve transection. The right and left LGd in a single tissue section are shown stained for NAAG in A and B. The loss of NAAG-IR in the neuropil of the LGd contralateral to the cut optic nerve was substantial (A). In hooded rats, two distinct patches of NAAG-IR puncta remained in the core region of the contralateral LGd that receives input from the ipsilateral eye (arrows in A). The area indicated by the upper arrow in A is shown at higher magnification in C. The homotopic regions in the opposite LGd contained only sparse NAAG-IR puncta (arrows in B), representing loss of the ipsilateral component of the retinogeniculate projection. The surrounding shell of the LGd retained its strong NAAG-immunoreactive afferentation (the area indicated by the upper arrow in B is shown at higher magnification in D). Images of the right and left LGd from a serial tissue section are shown stained for GAD_{67}-IR in E and F. GAD_{67}-IR was nearly absent in the axons of the optic tracts (see outer edges of LGd in E and F), but a few scattered immunoreactive neurons were seen within the tracts. Ten days after the unilateral optic nerve transection, a modest reduction in the intensity of GAD_{67}-IR was observed in the dorsal LGd (E). In hooded rats, a patch of higher GAD_{67}-IR was observed in the core of the LGd contralateral to the cut optic nerve (arrow in E, higher magnification in G). This is the region still receiving input from the intact ipsilateral optic nerve and is in the same position as the patch observed with NAAG-IR puncta noted above (cf. A and E). A very small loss of GAD_{67}-IR occurred in the core of the opposite LGd (arrow in F). This loss was more readily discernible at higher magnification (H). Scale bar = 300 μm for A,B,E,F, 50 μm for C,D,G,H.

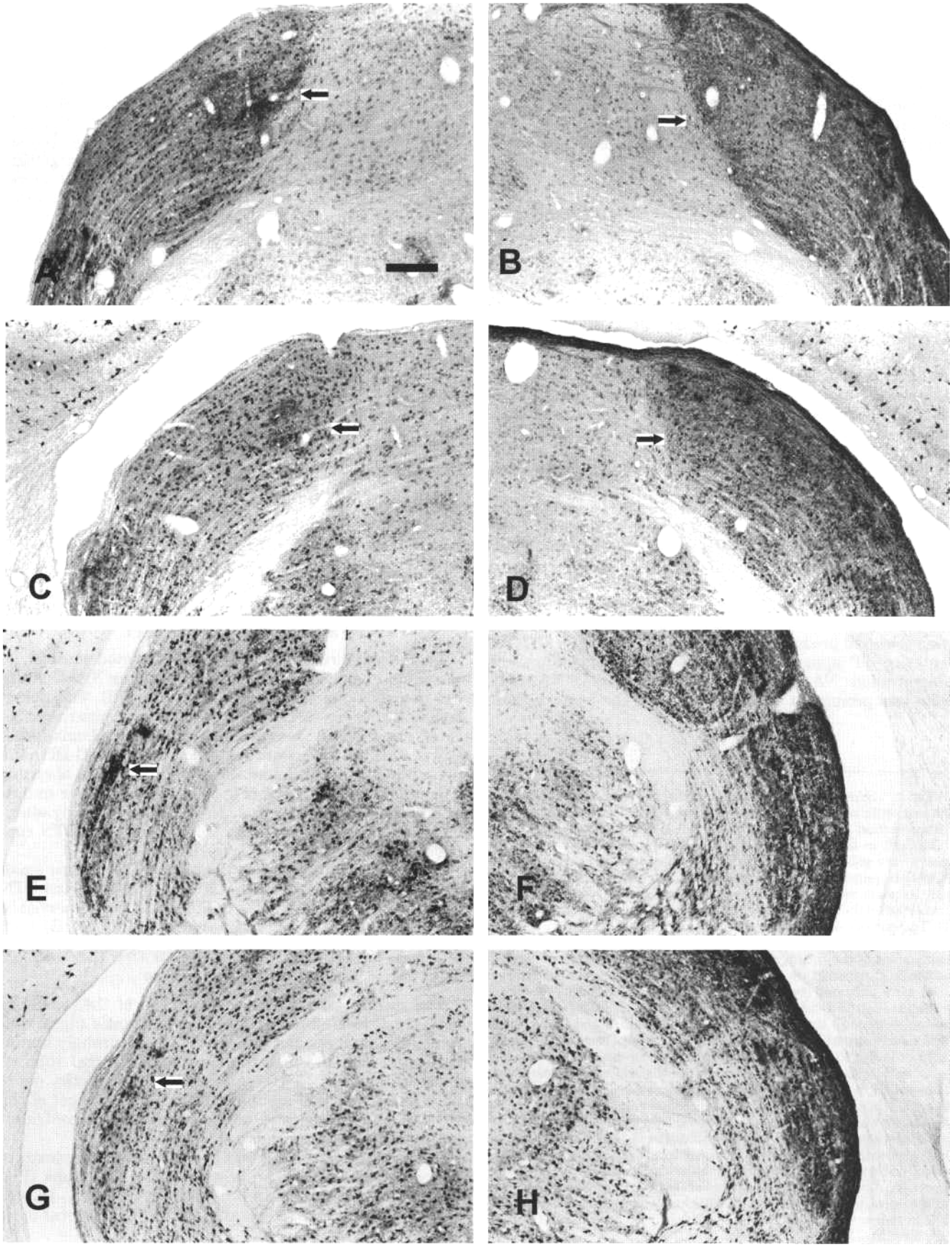

Figure 5

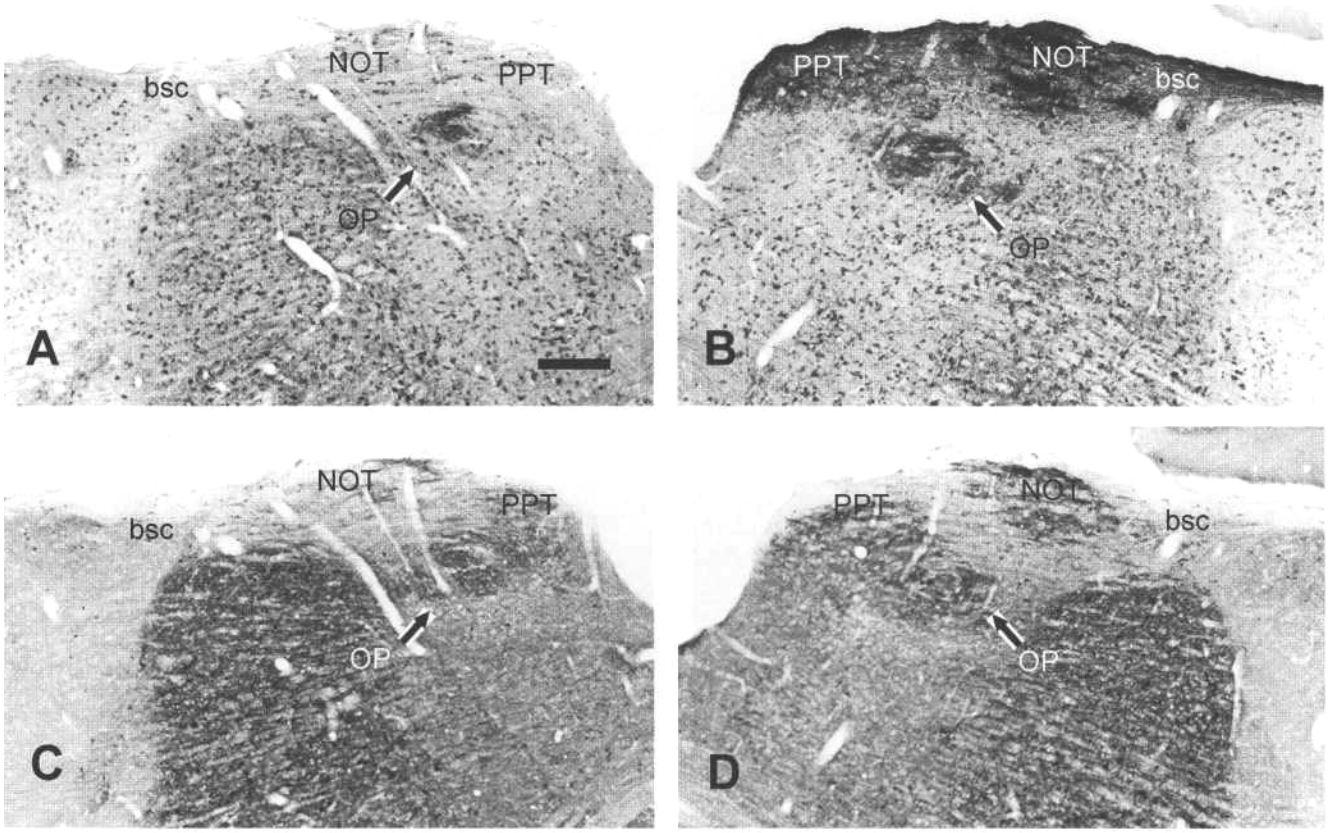

Fig. 6. NAAG-IR and GAD_{67}-IR in the pretectal nuclei, including OP, PPT, and NOT. NAAG-IR is shown in the right and left pretectal areas from a hooded rat (A,B) 10 days after a unilateral optic nerve transection. NAAG-IR axons of the brachium of the superior colliculus (bsc) were observed distributing immunopositive terminals to the pretectal nuclei (B). A moderate loss of NAAG-IR puncta was observed in the OP contralateral to the cut optic nerve, but a patch of NAAG-stained puncta remained (arrows). The loss of NAAG-IR puncta in the PPT and NOT contralateral to the cut nerve was almost complete (A). GAD_{67}-IR in the right and left pretectal areas from a tissue section adjacent to the one above is shown (C,D). Ten days after unilateral optic nerve transection, a moderate reduction in GAD_{67}-IR was observed in the NOT contralateral to the cut nerve, but no significant reduction was observed in the OP and PPT (C). Scale bar = 300 μm.

Superior colliculus

NAAG-IR was prominent in the retinorecipient layers of the superior colliculus (SC; right side of Fig. 9A,C,E). Strongly stained fibers could be seen coursing from the optic nerve fiber layer (op) to the superficial gray (sg) and zonal (zo) layers of the SC, where the neuropil was heavily labeled. This labeling decreased dramatically in the sg and zo layers contralateral to the cut nerve in animals with unilateral optic nerve transection (left side of Fig. 9A,C,E). Some of the small neurons in the outer zo and sg layers were NAAG positive (Fig. 9E), as were a few small and medium-sized neurons within the op layer. Many neurons in all sublayers of the intermediate gray were immunoreactive for NAAG, large multipolar neurons of layer b having the highest level of staining. Substantial numbers of the neurons of the SC deep gray and the adjacent periaqueductal gray were also moderately to strongly immunoreactive for NAAG.

No change in the density of NAAG-immunoreactive puncta was observed in the intermediate gray layers after unilateral or bilateral optic nerve transections. A very small proportion of NAAG-IR fibers remained in the op layer in animals with bilateral optic nerve transections. Because no NAAG-immunoreactive fibers remained in the optic nerves of animals with bilateral optic nerve transections, it seems likely that the remaining NAAG-positive fibers seen in the SC of animals with bilateral transections arise from an extraretinal source.

GAD_{67}-IR in the SC was prominent in a dense network of fine fibers and puncta in the sg and zo layers (Fig. 9B,D,F). The somata of marginal neurons and scattered

Fig. 5. Retinogeniculate projections in pigmented vs. albino rats. The distinct patterns of NAAG-IR in the right and left LGd of a pigmented rat (A,B) and an albino rat (C,D) are shown 10 days after unilateral optic nerve transections. In the LGd of the pigmented rat, the characteristic pattern of "core" and "shell" terminal distribution from opposing eyes was very evident (A,B). This distribution pattern for NAAG-IR was less obvious in the LGd of the albino rat 10 days after the transection but could still be discerned (C,D). The core termination zones that receive input from the ipsilateral eye are indicated by arrows in A-D. NAAG-IR in the right and left LGv of a hooded rat (E,F) and an albino rat (G,H) is shown 10 days following a unilateral optic nerve transection. Viewed in coronal sections, a vertical strip of NAAG-IR puncta remained in the lateral LGv, contralateral to the cut optic nerve. This NAAG-IR terminal zone was significantly denser in hooded rats (arrow in E) than in albino rats (arrow in G). Scale bar = 300 μm.

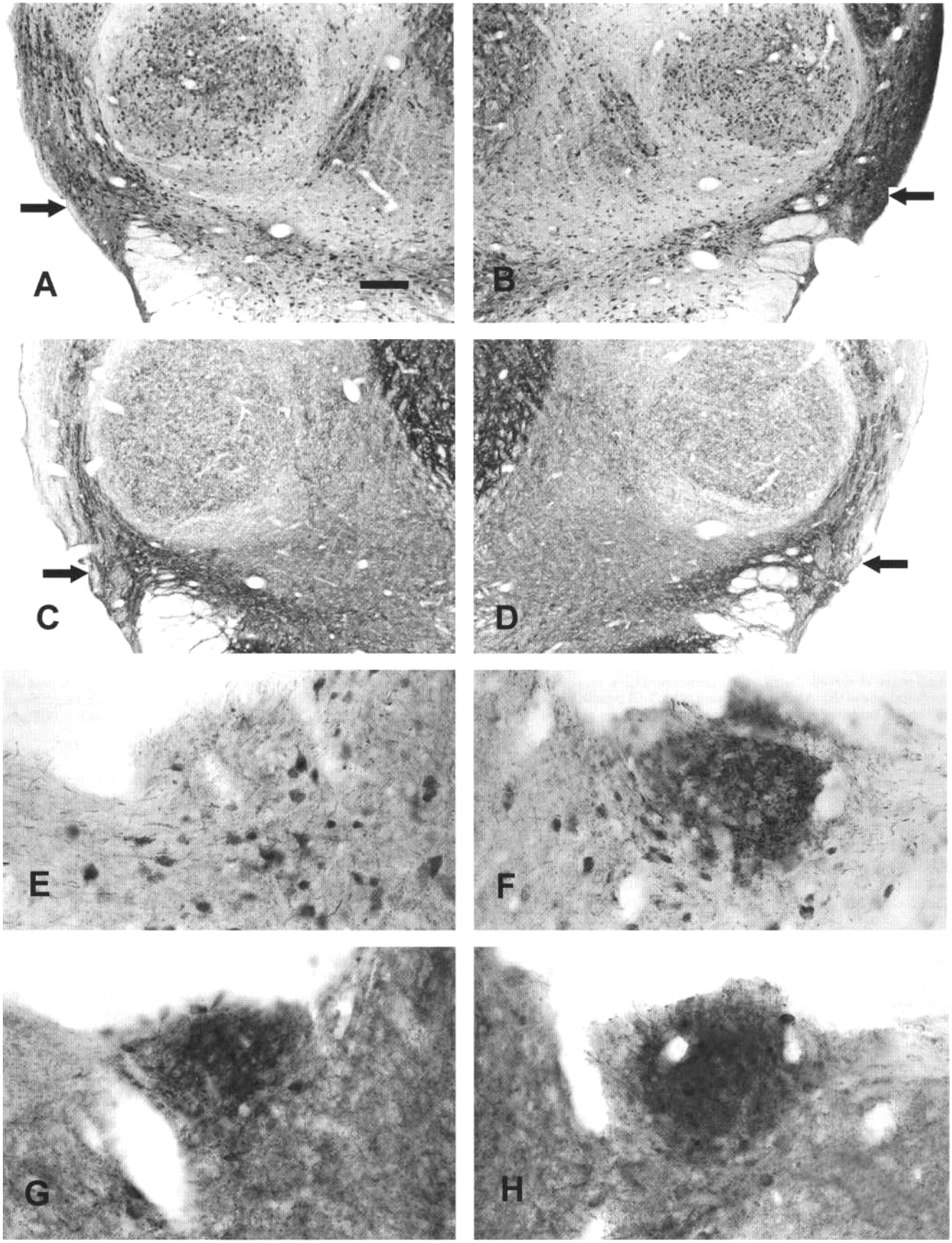

Figure 7

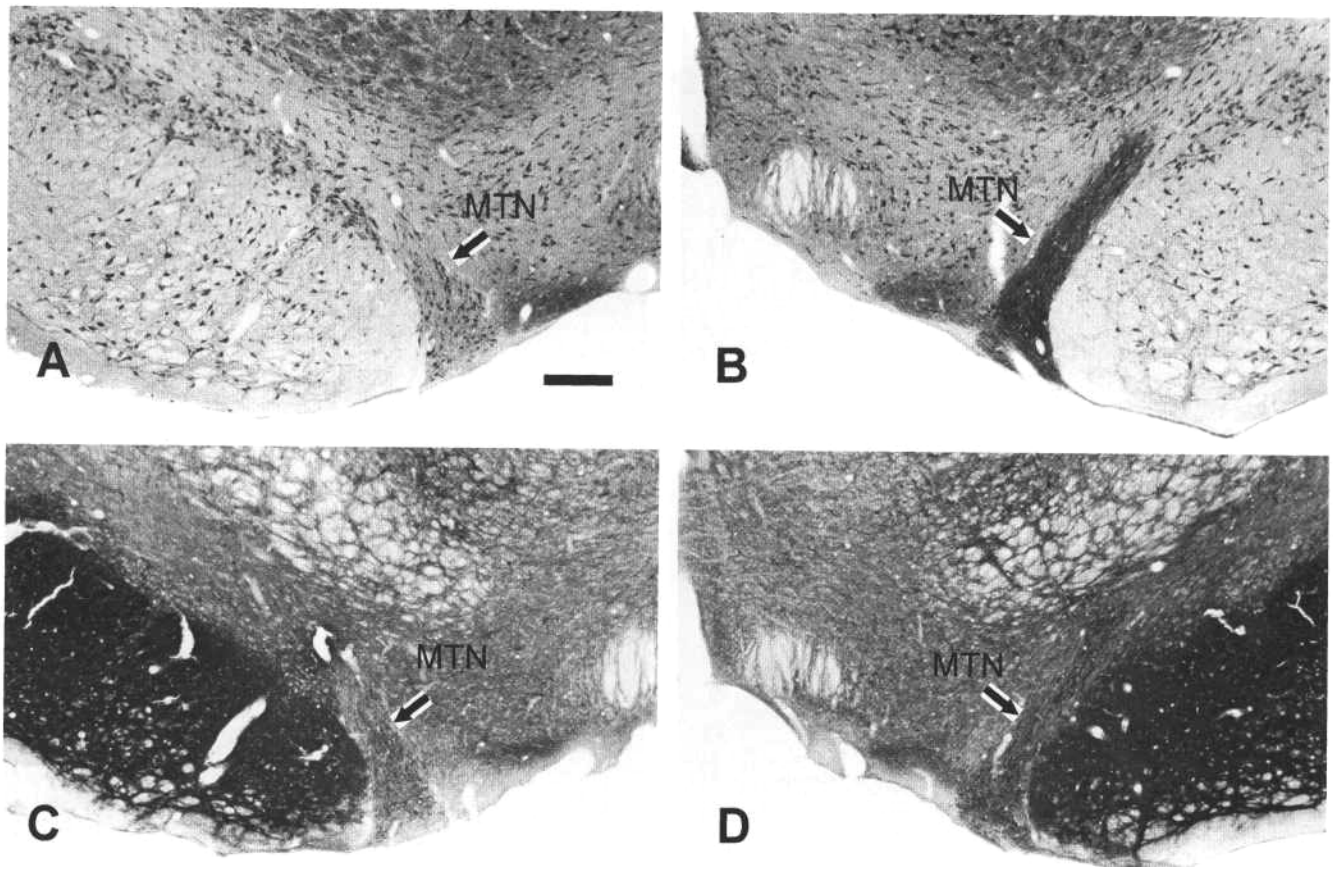

Fig. 8. NAAG-IR and GAD-IR in the MTN. Many fibers and puncta in the neuropil of the MTN were strongly immunoreactive for NAAG (B). This immunoreactivity was eliminated following deafferentation by optic nerve section (A). Neurons were also strongly labeled for NAAG in the MTN, but their labeling was masked by the intense fiber and terminal labeling in the afferented MTN. GAD_{67}-IR in the MTN was similarly present in a plexus of fibers and puncta and in some small neuronal cell bodies (C,D). Loss of GAD_{67}-IR was minor, but evident, in the MTN contralateral to the cut optic nerve (C). Scale bar = 100 μm.

neurons in the sg were immunoreactive for GAD_{67}. Some of the neurons in the op layer were strongly stained for GAD_{67}, as were some neurons in the intermediate and deep gray layers of the SC. GAD_{67}-IR in the neuropil of the intermediate and deep gray was less dense than that observed in the superficial retinorecipient layers. Ten days after unilateral optic nerve transection, a slight reduction in GAD_{67}-IR was observed in the contralateral sg layer (Fig. 9B,D,F). This reduction occurred in all GAD_{67}-immunoreactive stained elements, including the somata of interneurons and their associated fibers and synapses.

Fig. 7. NAAG-IR and GAD_{67}-IR in the lateral and dorsal terminal nuclei (LTN and DTN, respectively). The LTN (arrows in A-D) contained NAAG-IR fibers, puncta, and somata (B). Ten days after unilateral optic nerve transection, NAAG-IR was greatly reduced in the fibers and synapses in the contralateral LTN (A). Strong NAAG-IR was observed in the neuropil and in scattered neurons of the DTN (F). Deafferentation almost eliminated NAAG-IR in the neuropil of the DTN contralateral to the cut nerve (E). The LTN also contained GAD_{67}-IR in the neuropil and in some neuronal somata (D). No differences were noted in GAD_{67} staining in the LTN between innervated and denervated sides (cf. C and D). GAD_{67}-IR in the DTN was present in a dense accumulation of fine fibers and puncta as well as in some neuronal somata in and around the nucleus (H). Deafferentation made little or no difference in the intensity of GAD_{67}-IR in the DTN (cf. G and H). Scale bar = 300 μn for A-D, 50 μm for E-H.

NAAG-IR and GAD_{67}-IR double-labeling experiments

Double-labeling experiments in the rat retina demonstrated little or no NAAG and GAD_{67} colocalization in the ganglion cell layer. Most ganglion cells contained NAAG-IR in their somata, whereas GAD_{67}-IR in this layer appeared to be on the surface of the neurons (Fig. 10A). Some of the cells with GAD_{67}-IR in the ganglion cell layer could have been displaced amacrine cells. In contrast to the ganglion cell layer, some neurons in the inner nuclear layer of the retina were doubly stained for NAAG and GAD_{67} (Fig. 10B). NAAG-immunoreactive neurons outnumbered GAD_{67}-immunoreactive neurons in the inner nuclear layer, such that many of the NAAG-immunoreactive neurons in this layer were not doubly stained with antibodies to GAD_{67}.

In the rat LGd, NAAG-IR and GAD_{67}-IR were observed in distinct synaptic and neuronal populations (Fig. 10C-E). The somata of principal LGd neurons were lightly to moderately immunoreactive for NAAG but not for GAD_{67}.

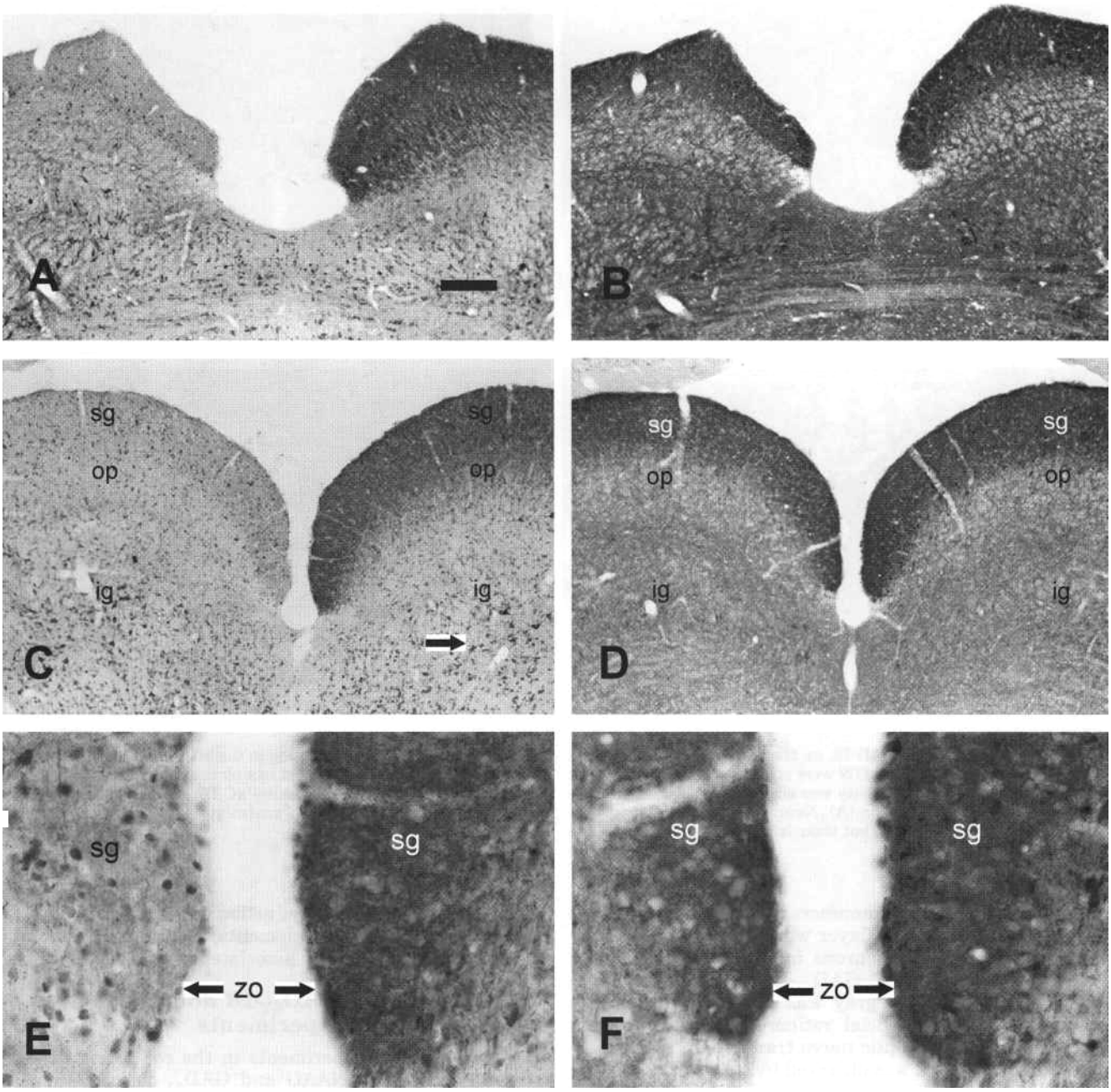

Fig. 9. NAAG-IR (left column) and GAD_{67}-IR (right column) in the hooded rat superior colliculus (SC) after unilateral optic nerve transection. The right side of each section received retinal input, whereas the left side of each section was deafferented. On the side receiving retinal input, NAAG-IR fibers can be seen coursing from the optic nerve (op) layer to the superficial gray (sg) and zonal (zo) layers (A,C,E). The anterior SC is shown stained for NAAG (A) and GAD_{67} (B) 10 days after unilateral transection. More caudal sections of the SC are shown stained for NAAG and GAD_{67} in C and D, and higher magnifications of these sections are shown in E and F. Many of the small marginal cells in the zo layer contained light to moderate NAAG-IR (E). Scattered neurons in the sg and op layers were moderately immunoreactive for NAAG. Neurons in all sublayers of the intermediate gray (ig) were immunoreactive for NAAG, with the most intense staining occurring in the large multipolar neurons of layer b (arrow in C). Neurons in the SC deep gray and the adjacent periaqueductal gray were also moderately to strongly immunoreactive for NAAG. Note the dramatic loss of NAAG-immunoreactive fibers and puncta in the sg and zo layers contralateral to the cut nerve (left side in A,C,E). GAD_{67}-IR in the SC was prominent in a dense network of fine fibers and puncta in the sg and zo layers (B,D,F). The somata of marginal neurons and scattered neurons in the sg layer were immunoreactive for GAD_{67}. Some of the neurons in the op layer were strongly stained for GAD_{67}, as were some neurons in the ig and deep gray. Ten days after unilateral optic nerve transection, a slight reduction in GAD_{67}-IR was observed in the contralateral sg layer of the SC (B,D,F; left side of each section). Scale bar = 300 μm for A-D, 50 μm for E,F.

In contrast, LGd interneurons, which could be distinguished by their smaller somata, were stained for GAD_{67} but not for NAAG (Fig. 10E). Immunostaining of axons and synaptic profiles with the two antibodies was also distinct in the LGd (Fig. 10E). Large-caliber axons within the LGd, primarily of retinal origin, were immunoreactive for NAAG, whereas small-caliber fibers within the LGd neuropil were immunoreactive for GAD_{67}. Despite the fact that the somata of LGd principal neurons were moderately to strongly NAAG positive, the axons of these cells were not immunoreactive for NAAG.

The thalamic reticular nucleus (TRN), located adjacent to the lateral geniculate nucleus, contains GABAergic neurons that project to and regulate the activity in the LG. Double-labeling experiments demonstrated that NAAG and GAD_{67} were present at high levels in most or all neurons of the TRN (Fig. 10F). NAAG-IR was observed only in the somata and proximal dendrites of TRN neurons, whereas GAD_{67}-IR was observed throughout TRN somata, processes, and terminals. This being the case, most processes in the TRN were labeled for GAD_{67} only. This included the axons of TRN neurons entering the internal capsule, which were stained for GAD_{67} but were always unstained for NAAG.

In the MTN, as in the LGd, NAAG-IR and GAD_{67}-IR were present in distinct neuronal elements. In the afferented MTN, NAAG-IR was observed in a dense plexus of afferent fibers and apparent synaptic endings that obscured most GAD_{67}-IR (Fig. 10H). Almost all of the NAAG-IR in the neuropil was lost contralaterally to the cut nerve after a unilateral optic nerve transection, revealing the NAAG-immunoreactive somata of principal MTN neurons and GAD_{67}-immunoreactive fibers and puncta present in the nucleus (Fig. 10G).

Because both primary antibodies used in these experiments were raised in rabbits and both were detected with similar goat anti-rabbit secondary antibodies, additional control experiments were performed. Their purpose was to determine whether the enzyme-labeled secondary antibody used to visualize the GAD_{67} antibodies in the second stage of labeling would detect the NAAG antibodies used in the first step of labeling. It was found that, when the first chromogen and second primary antibody steps were both omitted from double-labeling experiments, no anti-NAAG antibodies were detected with 5 μg/ml HRP-labeled goat anti-rabbit antibodies applied in the second stage of labeling. This control measure, in conjunction with the other control tests performed routinely (Moffett and Namboodiri, 1995), demonstrated that double-stained cells did in fact contain both antigens.

DISCUSSION

The visual projection system is notable among forebrain regions for its high NAAG content. In general, NAAG-IR in the rat forebrain does not correlate well with putative glutamatergic systems (Moffett et al., 1991b, 1993; Moffett and Namboodiri, 1995), one of the major exceptions being the retinal projections. NAAG-IR has been observed in the majority of retinal ganglion cells in every avian and mammalian species studied to date and is found in retinal terminals in all visual target areas (Tieman et al., 1987, 1988, 1991b; Moffett et al., 1990, 1991a; Williamson et al., 1991; Molinar-Rode and Pasik, 1992; Tieman and Tieman, 1996). Despite its phylogenetically conserved nature, the role of NAAG in the primary visual projections is unclear; electrophysiological investigations with NAAG application have yielded variable results (Jones and Sillito, 1992). Additionally, the favored transmitter candidate for the retinal projections, glutamate, is also present in the majority of retinal terminals (Montero, 1990; Cardozo et al., 1991). Whether NAAG and glutamate are localized in the same or distinct retinal terminals remains to be determined, but it seems likely that they are colocalized. The precise intracellular localization of NAAG in neurons is uncertain, but the fact that NAAG is released in a calcium-dependent manner (Williamson and Neale, 1988; Tsai et al., 1988; Zollinger et al., 1988; Williamson et al., 1991) suggests that NAAG is localized within synaptic vesicles. It is possible that NAAG, as with many peptides, is stored in dense core vesicles and is released differentially with respect to glutamate, depending on the degree or duration of depolarization. Dense core vesicles in the retinal projections are known to contain other peptides, such as substance P (Berg et al., 2000). The carbodiimide fixation method required for this study did not preserve ultrastructural cellular detail and, therefore, could not be used for electron microscopic immunocytochemistry to determine the intracellular localization of NAAG in retinal terminals.

NAAG has been shown to have numerous distinct actions in different experimental paradigms. These actions include selective interaction with the NMDA-type of glutamate receptor (Valivullah et al., 1994); direct, albeit relatively weak, postsynaptic excitatory effects on NMDA receptor-containing neurons (Westbrook et al., 1986; Trombley and Westbrook, 1990; Sekiguchi et al., 1992); modulation of neurotransmitter release (Galli et al., 1991; Puttfarcken et al., 1993, Zhao et al., 2001; Xi et al., 2002); inhibition of cAMP formation via metabotropic glutamate receptors (Wroblewska et al., 1993); enhancement of glutamate-mediated excitatory responses (Bos and Mirmiran, 1993); and reduction of stimulus-induced long-term potentiation of inhibitory postsynaptic potentials in the hippocampus (Lea et al., 2001). NAAG also has been found to be neuroprotective when the enzyme that degrades it in vivo is inhibited (Bruno et al., 1998a; Lu et al., 2000; Thomas et al., 2000). Extracellular NAAG can also act at metabotropic glutamate receptors on astrocytes (Haak et al., 1997; Wroblewska et al., 1998), resulting in the release of neuroprotective molecules, including transforming growth factor-B (Bruno et al., 1998b). It is evident from such findings that NAAG application does not always mimic the actions of glutamate, suggesting that its hydrolysis to glutamate is not a satisfactory explanation for the mechanisms of action of NAAG in the nervous system. Analysis of the ability of NAAG to activate cells transfected with metabotropic glutamate receptor subtypes 1-6 (mGluRl-6) has shown that NAAG is a selective agonist at the mGluR3 subtype (Wroblewska et al., 1997; Schweitzer et al., 2000). The mGluR3 receptor is negatively linked to adenylate cyclase and is most likely involved in the presynaptic regulation of transmitter release (Neale et al., 2000).

To determine whether NAAG and GAD_{67} were present in the same or in distinct neuronal populations, double-labeling experiments were performed with tissue from control animals and animals with unilateral or bilateral optic nerve transections. Colocalization studies demonstrated that the staining for NAAG and GAD_{67} was, in the

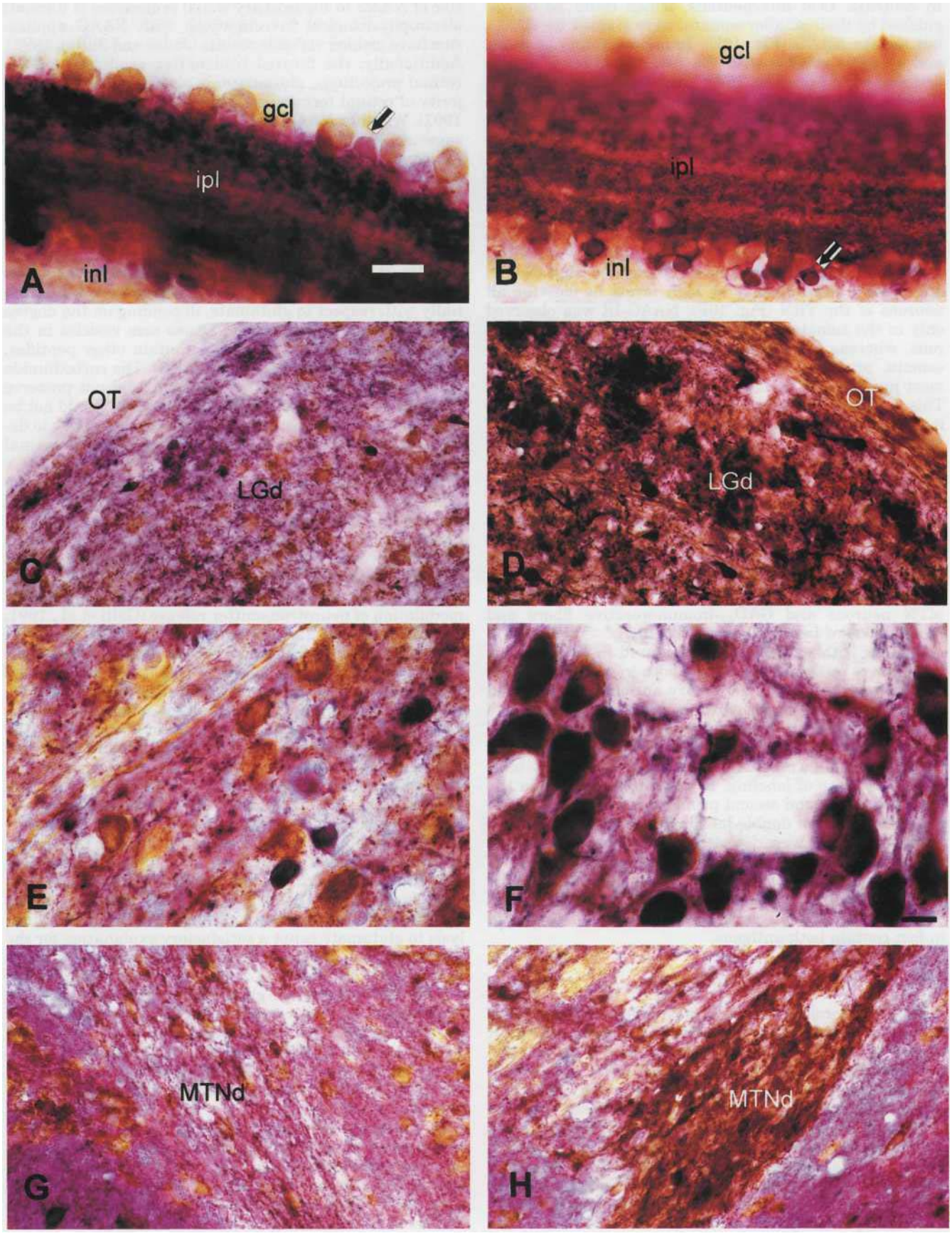

Figure 10

majority of cases, associated with different neuronal populations, confirming earlier findings in the cat (Xing and Tieman, 1993). In addition to being present in different types of neuronal somata, immunoreactivities for NAAG and GAD_{67} were present in distinct, dense networks of fibers and puncta in many visual target areas. These areas included the LGd, LGv, pretectal nuclei, terminal accessory nuclei, and superficial layers of the superior colliculus. In all these areas, most neurons, fibers, and puncta were not doubly stained for the two markers, but dense networks of distinct NAAG- and GAD_{67}-immunoreactive fibers and puncta were present. Often, adjacent brain areas not associated with the visual system had far less immunoreactivity for both markers in the neuropil. These findings are suggestive of unusually strong neurochemical interactions between NAAG and GABA in the visual system.

The thalamic reticular nucleus was unique among visual system-related areas in the complete colocalization of NAAG-IR and GAD_{67}-IR in neuronal cell bodies. This has been shown previously in the cat (Xing and Tieman, 1993). A similar observation has been made with antibodies to GABA, glutamate, and aspartate; most or all rat TRN neurons were found to be doubly labeled for GABA and either glutamate or aspartate (Gonzalo-Ruiz et al., 1996). In the present study, GAD_{67}-IR was observed throughout the somata, dendrites, and axonal projections of TRN neurons, but NAAG-IR was present only in TRN somata and proximal dendrites. Confinement of NAAG-IR to the soma and proximal dendrites has been reported for other GABAergic projection neurons, such as those of the globus pallidus, and the reticular portion of the substantia nigra (Moffett and Namboodiri, 1995). It is possible, based on these observations, that NAAG synthesized in the TRN and other GABAergic systems is released locally from somata and basal dendrites rather than at axonal terminals. This would be in clear distinction to glutamatergic systems, such as the retinal projections, where NAAG-IR is found throughout the axons and terminal fields and is known to be released in a calcium-dependent manner (Williamson et al., 1991).

In the present study, there were instances in which known glutamatergic systems exhibited NAAG-IR that was restricted to cell bodies and basal dendrites, including principal neurons of the LGd. Similarly to the case in the TRN, which lacked NAAG-IR in the efferent projections, no NAAG-IR was seen in the thalamocortical radiation from LGd to occipital cortex. With these observations, it seems useful to define two types of NAAG localization: type 1, in which cell bodies, basal dendrites, axons, and terminals are all immunoreactive, and type 2, in which only cell bodies and basal dendrites contain NAAG. The type 1 pattern is associated more with excitatory pathways, such as the ganglion cell layer of the retina, whereas the type 2 pattern is associated more with inhibitory neuron systems, such as the TRN. The LGd of the rat was one exception in the current study, in which principal neurons had the type 2 pattern of NAAG-IR despite the use of glutamate as the neurotransmitter.

It is possible to begin constructing scenarios for the action of NAAG in the visual projections based on anatomical, pharmacological, and physiological data. The discussion below uses the LGd as an example. One type of synaptic complex in the LGd is the triadic synaptic arrangement on the dendritic spines of thalamocortical projection neurons. These glomerular synapses include excitatory afferent terminals from both the retina and the occipital cortex as well as inhibitory terminals from GABAergic neurons in the LGd and TRN, all impinging on single LGd neuronal dendritic spines. NAAG could act through presynaptic mGluR3 receptors to modulate either glutamate release from cortical and retinal afferents or GABA release from the inhibitory fibers, or both. Because NAAG is known to inhibit GABA release by cortical neurons (Zhao et al., 2001), it is possible that NAAG would have the same effect on GABA release within the LGd. Recent evidence indicates that NAAG inhibits both vesicular and nonvesicular glutamate release and reduces extracellular glutamate levels in the nucleus accumbens (Xi et al., 2002). It is therefore possible that NAAG inhibits both GABA and glutamate release in the LGd triadic synaptic complex, where retinal fibers make contact with LGd neurons. One of the functions of NAAG in the visual projections could be to make the retinogeniculate transmission process more discrete, by limiting further transmitter release after exocytosis is initiated via depolarization. The glomerular synaptic arrangement would allow NAAG released at ganglion cell terminals to act on presynaptic terminals originating in the retina, cortex, TRN, and local inhibitory neurons.

Glutamate is released continuously during extended periods of activity in retinal target areas, such as the LGd and superior colliculus. This chronic glutamate release may require special mechanisms to protect postsynaptic retinal target neurons from excitotoxic stress during periods of prolonged activity. The dense plexus of NAAG- and GABA-containing fibers and terminals observed in many retinal target areas may subserve this function. NAAG could act in an autoregulatory role at retinal terminals, limiting glutamate release, with subsequent local GABA release acting to hyperpolarize postsynaptic principal neurons. This would be in accordance with NAAG's known

Fig. 10. Double-labeling experiments demonstrated that NAAG-IR (orange/brown) and GAD_{67}-IR (purple) in the retina were partially colocalized. Many ganglion cells contained varying degrees of NAAG-IR. In contrast, very few cells in the ganglion cell layer (gel) contained significant amounts of GAD_{67}-IR, and these appeared to express GAD staining predominantly on their surface, giving them a very light purple appearance (arrow in A). Some cells in the inner nuclear layer (inl) were doubly stained for NAAG and GAD_{67} (arrow in B), but most stained neurons in this layer were singly labeled for NAAG (B). In the LGd and all retinorecipient zones, NAAG-IR and GAD_{67}-IR were observed in distinct synaptic and neuronal populations (C—E,G,H). Principal LG neurons with large somata were lightly to moderately immunoreactive for NAAG (orange/brown in E) but not for GAD_{67} (purple). In contrast, small LGd interneurons were stained for GAD_{67} but not for NAAG (E). The strong NAAG-IR observed in fibers and puncta in the innervated LGd (D) was absent in the deafferented LGd (C). Small GAD_{67}-immunoreactive somata, as well as dendrites, axons, and terminals, were still visible throughout the LGd after optic nerve transection (E). Double-labeling experiments demonstrated that NAAG-IR and GAD_{67}-IR were present at high levels in most or all neurons of the thalamic reticular nucleus (TRN), giving the neuronal somata a brown/black appearance (F). In the dorsal MTN (MTNd), NAAG-IR and GAD_{67}-IR were present in distinct neuronal and neuropil elements. The right and left MTNd from a hooded rat are shown after a unilateral optic nerve transection. The strong NAAG-IR present in the neuropil ipsilateral to the cut optic nerve (H) was absent contralaterally to the cut nerve (G). Scale bar = 20 μm for A,B,E,F, 50 μm for C,D,G,H.

neuroprotective actions and could explain the extensive colocalization of NAAG and GAD_{67} in the retinal target areas (Bruno et al., 1998a; Lu et al., 2000; Thomas et al., 2000). If NAAG is indeed present in dense core vesicles and is released only when ganglion cell terminal depolarization is prolonged, its function may be to prevent overexcitation of postsynaptic, retinoreceptive neurons by keeping glutamate release in check.

Lamination in the LGd occurs in animals with binocular vision. Retinal inputs to adjacent layers come from opposite eyes and provide for overlapping representation of the visual information from each eye in the binocular visual field. Rats have a relatively small binocular portion of their visual field, and this is reflected in the relatively minor ipsilateral projecting component of the retinal efferents. Nonetheless, the portion of the temporal retina that is in the binocular field of vision does send a small projection to the core of the ipsilateral LGd, and this component is noticeably more robust in hooded rats than in albino rats. Therefore, after a unilateral optic nerve transection, a patch of retinal terminals remains in the core of the LGd ipsilateral to the intact nerve, and this patch contains more retinal terminals in pigmented rats than in albino rats. The results of the present study clearly demonstrated this arrangement in hooded and albino rats by using antibodies to NAAG. Reese (1988) has shown that there is anatomical evidence for the apposition of the representation of the conjugate retinal inputs in the rat LGd, although it is relatively minor compared with that in carnivores and primates. The present results show the segregation of ocularly distinct afferents to the core and shell of the rat LGd based on the presence of a neuroactive compound and support the concept that the retinotopic maps in the binocular field are in register. Previous enucleation studies have demonstrated the loss of the ipsilateral and contralateral components of the visual projections in the cat LGd using antibodies to NAAG (Tieman et al., 1991b).

Transynaptic reductions in the level of GAD_{67}-IR were observed in many retinal targets 10 days after optic nerve transections. These changes were much less dramatic than those associated with the direct loss of NAAG in retinal fibers and terminals. However, the loss could be discerned within a single LGd from animals with a unilateral optic nerve transection by comparing the areas that receive ipsilateral and contralateral retinal input. Although any account of these findings involves speculation, it is known that increased intracellular concentrations of GABA lead to significant reductions in GAD_{67} protein content in GABAergic neurons (Rimvall and Martin, 1992, 1994; Rimvall et al., 1993). It is possible that reduced glutamate release in the LGd after optic nerve transection contributes to the transynaptic drop observed in GAD_{67}-IR. The loss of glutamatergic stimulation of the GABAergic cells would lead to a buildup in intracellular GABA concentrations in these LGd interneurons. This increase in intracellular GABA content could then lead to the reduction in observable GAD_{67} levels in these cells.

Even though there is no evidence linking NAAG directly to changes in GAD_{67} expression, a direct effect of NAAG on GABA receptor subunit expression has been shown. Application of NAAG to cerebellar granule cell cultures leads to a transient increase in GABA(A) alpha-6 subunit mRNA and a fourfold increase in alpha-6 protein content (Ghose et al., 1997). Up-regulation of GABA receptor expression in response to NAAG release may have long-term neuroprotective effects. Clearly, NAAG is a multifunctional compound with unique actions that distinguish it from excitatory neurotransmitters. The precise functional interactions between NAAG and GABA in the visual system, and throughout the CNS, are topics for future research.

ACKNOWLEDGMENTS

The author thanks Dr. Joseph H. Neale, without whom this work would not have been possible, and Drs. M.A. Namboodiri, Douglas A. Eagles, and Miriam LeGare for assistance, essential discussions, and support.

LITERATURE CITED

Anderson KJ, Borja MA, Cotman CW, Moffett JR, Namboodiri MA, Neale JH. 1987. N-acetylaspartylglutamate identified in the rat retinal ganglion cells and their projections in the brain. Brain Res 411:172—177.

Berg EA, Johnson RJ, Leeman SE, Boyd N, Kimerer L, Fine RE. 2000. Isolation and characterization of substance P-containing dense core vesicles from rabbit optic nerve and termini. J Neurosci Res 62:830-839.

Bos NPA, Mirmiran M. 1993. Effects of excitatory and inhibitory amino acids on neuronal discharges in the cultured suprachiasmatic nucleus. Brain Res Bull 31:67-72.

Bruno V, Wroblewska B, Wroblewski JT, Fiore L, Nicoletti F. 1998a. Neuroprotective activity of N-acetylaspartylglutamate in cultured cortical cells. Neuroscience 85:751-757.

Bruno V, Battaglia G, Casabona G, Copani A, Caciagli F, Nicoletti F. 1998b. Neuroprotection by glial metabotropic glutamate receptors is mediated by transforming growth factor-beta. J Neurosci 18:9594-9600.

Cardozo BN, Buijs R, Van der Want J. 1991. Glutamate-like immunoreactivity in retinal terminals in the nucleus of the optic tract in rabbits. J Comp Neurol 309:261-270.

Crunelli V, Kelly JS, Leresche N, Pirchio M. 1987. On the excitatory postsynaptic potential evoked by stimulation of the optic tract in the rat lateral geniculate nucleus. J Physiol (London) 384:603—618.

Funke K, Eysel UT, FitzGibbon T. 1991. Retinogeniculate transmission by NMDA and non-NMDA receptors in the cat. Brain Res 547:229-238.

Galli T, Godeheu G, Artaud F, Desce JM, Pittaluga A, Barbeito L, Glowinski J, Cheramy A. 1991. Specific role of N-acetyl-aspartyl-glutamate in the in vivo regulation of dopamine release from dendrites and nerve terminals of nigrostriatal dopaminergic neurons in the cat. Neuroscience 42:19-28.

Ghose S, Wroblewska B, Corsi L, Grayson DR, de Bias AL, Vicini S, Neale JH. 1997. N-acetylaspartylglutamate stimulates metabotropic glutamate receptor 3 to regulate expression of the GABA(A) alpha6 subunit in cerebellar granule cells. J Neurochem 69:2326—2335.

Gonzalo-Ruiz A, Sanz JM, Lieberman AR. 1996. Immunohistochemical studies of localization and colocalization of glutamate, aspartate, and GABA in the anterior thalamic nuclei, retrosplenial granular cortex, thalamic reticular nucleus, and mammillary nuclei of the rat. J Chem Neuroanat 12:77-84.

Haak LL, Heller HC, Van den Pol AN. 1997. Metabotropic glutamate receptor activation modulates kainate and serotonin calcium response in astrocytes. J Neurosci 17:1825-1837.

Henderson Z, Salt TE. 1988. The effects of N-acetylaspartylglutamate and distribution of N-acetylaspartylglutamate-like immunoreactivity in the rat somatosensory thalamus. Neuroscience 25:899—906.

Johnson RF, Morin LP, Moore RY. 1988. Retinohypothalamic projections in the hamster and rat demonstrated using cholera toxin. Brain Res 462:301-312.

Jones HE, Sillito AM. 1992. The action of the putative neurotransmitters N-acetylaspartylglutamate and L-homocysteate in cat dorsal lateral geniculate nucleus. J Neurophysiol 68:663-672.

Kemp JA, Sillito AM. 1982. The nature of the excitatory transmitter mediating X and Y cell inputs to the cat dorsal lateral geniculate nucleus. J Physiol (London) 323:377-391.

Kita H, Oomura Y. 1982. An anterograde HRP study of retinal projections to the hypothalamus in the rat. Brain Res Bull 8:249-253.

Lea PM, Wroblewska B, Sarvey JM, Neale JH. 2001. Beta-NAAG rescues LTP from blockade by NAAG in rat dentate gyrus via the type 3 metabotropic glutamate receptor. J Neurophysiol 85:1097-1106.

Lu XM, Tang Z, Liu W, Lin Q, Slusher BS. 2000. N-acetylaspartylglutamate protects against transient focal cerebral ischemia in rats. Eur J Pharmacol 408:233-239.

Moffett JR, Namboodiri MA. 1995. Differential distribution of N-acetylaspartylglutamate and N-acetylaspartate immunoreactivities in rat forebrain. J Neurocytol 24:409-433.

Moffett JR, Williamson LC, Palkovits M, Namboodiri MA. 1990. N-acetylaspartylglutamate: a transmitter candidate for the retinohypothalamic tract. Proc Natl Acad Sci USA 87:8065-8069.

Moffett JR, Namboodiri MA, Cangro CB, Neale JH. 1991a. Immunohistochemical localization of N-acetylaspartate in rat brain. Neuroreport 2:131-134.

Moffett JR, Williamson LC, Neale JH, Palkovits M, Namboodiri MA. 1991b. Effect of optic nerve transection on N-acetylaspartylglutamate immunoreactivity in the primary and accessory optic projection systems in the rat. Brain Res 538:86-94.

Moffett JR, Namboodiri MA, Neale JH. 1993. Enhanced carbodiimide fixation for immunohistochemistry: application to the comparative distributions of N-acetylaspartylglutamate and N-acetylaspartate immunoreactivities in rat brain. J Histochem Cytochem 41:559-570.

Moffett JR, Palkovits M, Namboodiri MA, Neale JH. 1994. Comparative distribution of N-acetylaspartylglutamate and GAD_{67} immunoreactivities in the cerebellum and precerebellar nuclei of the rat utilizing enhanced carbodiimide fixation and immunohistochemistry. J Comp Neurol 347:598-618.

Molinar-Rode R, Pasik P. 1992. Amino acids and N-acetyl-aspartylglutamate as neurotransmitter candidates in the monkey retinogeniculate pathways. Exp Brain Res 89:40-48.

Montero VM. 1990. Quantitative immunogold analysis reveals high glutamate levels in synaptic terminals of retino-geniculate, cortico-geniculate, and geniculo-cortical axons in the cat. Vis Neurosci 4:437-443.

Montero VM, Wenthold RJ. 1989. Quantitative immunogold analysis reveals high glutamate levels in retinal and cortical synaptic terminals in the lateral geniculate nucleus of the macaque. Neuroscience 31:639-647.

Moore RY, Speh JC. 1993. GABA is the principal neurotransmitter of the circadian system. Neurosci Lett 150:112-116.

Neale JH, Bzdega T, Wroblewska B. 2000. N-acetylaspartylglutamate: the most abundant peptide neurotransmitter in the mammalian central nervous system. J Neurochem 75:443-452.

Puttfarcken PS, Handen JS, Montgomery DT, Coyle JT, Werling LL. 1993. N-acetyl-aspartylglutamate modulation of N-methyl-D-aspartate-stimulated [^{3}H]norepinephrine release from rat hippocampal slices. J Pharmacol Exp Ther 266:796-803.

Radhakrishnan V, Henry JL. 1993. Excitatory amino acid receptor mediation of sensory inputs to functionally identified dorsal horn neurons in cat spinal cord. Neuroscience 55:531-544.

Reese BE. 1988. 'Hidden lamination' in the dorsal lateral geniculate nucleus: the functional organization of this thalamic region in the rat. Brain Res 472:119-137.

Rimvall K, Martin DL. 1992. Increased intracellular gamma-aminobutyric acid selectively lowers the level of the larger of two glutamate decarboxylase proteins in cultured GABAergic neurons from rat cerebral cortex. J Neurochem 58:158-166.

Rimvall K, Martin DL. 1994. The level of GAD_{67} protein is highly sensitive to small increases in intraneuronal gamma-aminobutyric acid levels. J Neurochem 62:1375-1381.

Rimvall K, Sheikh SN, Martin DL. 1993. Effects of increased gamma-aminobutyric acid levels on GAD_{67} protein and mRNA levels in rat cerebral cortex. J Neurochem 60:714-720.

Riveros N, Orrego F. 1984. A study of possible excitatory effects of N-acetylaspartylglutamate in different in vivo and in vitro brain preparations. Brain Res 299:393-395.

Schweitzer C, Kratzeisen C, Adam G, Lundstrom K, Malherbe P, Ohresser S, Stadler H, Wichmann J, Woltering T, Mutel V. 2000. Characterization of [(3)H]-LY354740 binding to rat mGlu2 and mGlu3 receptors expressed in CHO cells using semliki forest virus vectors. Neuropharmacology 39:1700-1706.

Sekiguchi M, Wada K, Wenthold RJ. 1992. N-acetylaspartylglutamate acts as an agonist upon homomeric NMD A receptor (NMDAR1) expressed in *Xenopus* oocytes. FEBS Lett 311:285-289.

Serval V, Barbeito L, Pittaluga A, Cheramy A, Lavielle S, Glowinski J. 1990. Competitive inhibition of N-acetylated-alpha-linked acidic dipeptidase activity by N-acetyl-L-aspartyl-beta-linked L-glutamate. J Neurochem 55:39-46.

Sillito AM, Murphy PC, Salt TE. 1990a. The contribution of the non-N-methyl-D-aspartate group of excitatory amino acid receptors to retinogeniculate transmission in the cat. Neuroscience 34:273-280.

Sillito AM, Murphy PC, Salt TE, Moody CI. 1990b. Dependence of retinogeniculate transmission in cat on NMDA receptors. J Neurophysiol 63:347-355.

Swanson LW. 1992. Brain maps: structure of the rat brain. Amsterdam: Elsevier.

Thomas AG, Vornov JJ, Olkowski JL, Merion AT, Slusher BS. 2000. N-acetylated alpha-linked acidic dipeptidase converts N- acetylaspartylglutamate from a neuroprotectant to a neurotoxin. J Pharmacol Exp Ther 295:16-22.

Tieman SB, Tieman DG. 1996. N-acetylaspartylglutamate immunoreactivity in human retina. Vis Res 36:941-947.

Tieman SB, Cangro CB, Neale JH. 1987. N-acetylaspartylglutamate immunoreactivity in neurons of the cat's visual system. Brain Res 420:188—193.

Tieman SB, Butler K, Neale JH. 1988. N-acetylaspartylglutamate. A neuropeptide in the human visual system. JAMA 259:2020.

Tieman SB, Neale JH, Tieman DG. 1991a. N-acetylaspartylglutamate immunoreactivity in neurons of the monkey's visual pathway. J Comp Neurol 313:45-64.

Tieman SB, Moffett JR, Irtenkauf SM. 1991b. Effect of eye removal on N-acetylaspartylglutamate immunoreactivity in retinal targets of the cat. Brain Res 562:318-322.

Trombley PQ, Westbrook GL. 1990. Excitatory synaptic transmission in cultures of rat olfactory bulb. J Neurophysiol 64:598-606.

Tsai G, Forloni GL, Robinson MB, Stauch BL, Coyle JT. 1988. Calcium-dependent evoked release of N-[^{3}H]acetylaspartylglutamate from the optic pathway. J Neurochem 51:1956-1959.

Valivullah HM, Lancaster J, Sweetnam PM, Neale JH. 1994. Interactions between N-acetylaspartylglutamate and AMPA, kianate and NMDA binding sites. J Neurochem 63:1714-1719.

Van den Pol AN. 1991. Glutamate and aspartate immunoreactivity in hypothalamic presynaptic axons. J Neurosci 11:2087-2101.

Westbrook GL, Mayer ML, Namboodiri MA, Neale JH. 1986. High concentrations of N-acetylaspartylglutamate (NAAG) selectively activate NMDA receptors on mouse spinal cord neurons in cell culture. J Neurosci 6:3385-3392.

Whittemore ER, Koerner JF. 1989. An explanation for the purported excitation of piriform cortical neurons by N-acetyl-L-aspartyl-L-glutamic acid (NAAG). Proc Natl Acad Sci USA 86:9602-9605.

Williamson LC, Neale JH. 1988. Calcium-dependent release of N-acetylaspartylglutamate from retinal neurons upon depolarization. Brain Res 475:151-155.

Williamson LC, Eagles DA, Brady MJ, Moffett JR, Namboodiri MA, Neale JH. 1991. Localization and synaptic release of N-acetylaspartylglutamate in the chick retina and optic tectum. Eur J Neurosci 3:441-451.

Wroblewska B, Wroblewski JT, Saab OH, Neale JH. 1993. N-acetylaspartylglutamate inhibits forskolin-stimulated cyclic AMP levels via a metabotropic glutamate receptor in cultured cerebellar granule cells. J Neurochem 61:943-948.

Wroblewska B, Wroblewski JT, Pshenichkin S, Surin A, Sullivan SE, Neale JH. 1997. N-acetylaspartylglutamate selectively activates mGluR3 receptors in transfected cells. J Neurochem 69:174—181.

Wroblewska B, Santi MR, Neale JH. 1998. N-acetylaspartylglutamate activates cyclic AMP-coupled metabotropic glutamate receptors in cerebellar astrocytes. Glia 24:172-179.

Xi ZX, Baker DA, Shen H, Carson DS, Kalivas PW. 2002. Group II metabotropic glutamate receptors modulate extracellular glutamate in the nucleus accumbens. J Pharmacol Exp Ther 300:162-171.

Xing LC, Tieman SB. 1993. Relay cells, not interneurons, of cat's lateral geniculate nucleus contain N-acetylaspartylglutamate. J Comp Neurol 330:272-285.

Yamamoto T, Nozaki-Taguchi N, Sakashita Y. 2001. Spinal N-acetyl-alpha-linked acidic dipeptidase (NAALADase) inhibition attenuates mechanical allodynia induced by paw carrageenan injection in the rat. Brain Res 909:138-144.

Zhao J, Ramadan E, Cappiello M, Wroblewska B, Bzdega T, Neale JH. 2001. NAAG inhibits KCl-induced [(3)H]-GABA release via mGluR3, cAMP, PKA and L-type calcium conductance. Eur J Neurosci 13:340-346.

Zollinger M, Amsler U, Do KQ, Streit P, Cuenod M. 1988. Release of N-acetylaspartylglutamate on depolarization of rat brain slices. J Neurochem 51:1919-1923.